Cell shape and antibiotic resistance is maintained by the activity of multiple FtsW and RodA enzymes in *Listeria monocytogenes*

Jeanine Rismondo[1], Sven Halbedel[2] and Angelika Gründling[1#]

[1] Section of Microbiology and Medical Research Council Centre for Molecular Bacteriology and Infection, Imperial College London, London SW7 2AZ.

[2] FG11 Division of Enteropathogenic bacteria and *Legionella*, Robert Koch-Institute, Burgstrasse 37, 38855 Wernigerode, Germany.

[#]To whom correspondence should be addressed: Angelika Gründling – a.grundling@imperial.ac.uk

Abstract word count: 250

Main text word count: 6801

Running Title: Functional analysis of multiple SEDS in *Listeria*

Abstract

Rod-shaped bacteria have two modes of peptidoglycan synthesis: lateral synthesis and synthesis at the cell division site. These two processes are controlled by two macromolecular protein complexes, the elongasome and divisome. Recently, it has been shown that the *Bacillus subtilis* RodA protein, which forms part of the elongasome, has peptidoglycan glycosyltransferase activity. The cell division specific RodA homolog FtsW fulfils a similar role at the divisome. The human pathogen *Listeria monocytogenes* encodes up to six FtsW/RodA homologs, however their functions have not yet been investigated. Analysis of deletion and depletion strains led to the identification of the essential cell division-specific FtsW protein, FtsW1. Interestingly, *L. monocytogenes* encodes a second FtsW protein, FtsW2, which can compensate for the lack of FtsW1, when expressed from an inducible promoter. *L. monocytogenes* also possesses three RodA homologs, RodA1, RodA2 and RodA3 and their combined absence is lethal. Cells of a *rodA1*/*rodA3* double mutant are shorter and have increased antibiotic and lysozyme sensitivity, probably due to a weakened cell wall. Results from promoter activity assays revealed that expression of *rodA3* and *ftsW2* is induced in the presence of antibiotics targeting penicillin binding proteins. Consistent with this, a *rodA3* mutant was more susceptible to the β-lactam antibiotic cefuroxime. Interestingly, overexpression of RodA3 also led to increased cefuroxime sensitivity. Our study highlights that *L. monocytogenes* encodes a multitude of functional FtsW and RodA enzymes to produce its rigid cell wall and that their expression needs to be tightly regulated to maintain growth, cell division and antibiotic resistance.

Importance

The human pathogen *Listeria monocytogenes* is usually treated with high doses of β-lactam antibiotics, often combined with gentamicin. However, these antibiotics only act bacteriostatically on *L. monocytogenes* and the immune system is needed to clear the infection. Therefore, individuals with a compromised immune system are at risk to develop a severe form of *Listeria* infection, which can be fatal in up to 30% of cases. The development of new strategies to treat *Listeria* infections is therefore necessary. Here we show that the expression of some of the FtsW and RodA enzymes of *L. monocytogenes* is induced by the presence of β-lactam antibiotics and their combined absence makes bacteria more susceptible to this class of antibiotics. The development of antimicrobials that inhibit the activity or production of FtsW/RodA enzymes might therefore help to improve the treatment of *Listeria* infections and thereby lead to a reduction in mortality.

64 **Introduction**

65 Bacterial cells are surrounded by a mesh of peptidoglycan (PG) that determines their shape
66 and also protects the cells from lysis due to their high internal turgor pressure (Weidel and
67 Pelzer, 1964, Vollmer et al., 2008, de Pedro and Cava, 2015). Peptidoglycan is comprised of
68 glycan strands that are crosslinked by short peptides (Rogers et al., 1980). The glycan strands
69 are composed of alternating N-acetylglucosamine and N-acetylmuramic acid residues that are
70 connected by a β-1,4 glycosidic bond (Ghuysen and Strominger, 1963). The synthesis of
71 peptidoglycan begins in the cytoplasm with the production of the PG precursor lipid II by the
72 proteins MurABCDEF, MraY and MurG (Blumberg and Strominger, 1974, van Heijenoort,
73 2001, Scheffers and Pinho, 2005, Pinho et al., 2013). Lipid II is then transported across the
74 cytoplasmic membrane by the flippase MurJ and Amj (Meeske et al., 2015, Sham et al.,
75 2014, Ruiz, 2008) and subsequently incorporated in the growing glycan strand by
76 glycosyltransferases. The polymerization and the crosslinking of the glycan strands are
77 facilitated by the activity of glycosyltransferases and transpeptidases, respectively. Class A
78 penicillin binding proteins (PBPs) are bifunctional enzymes that possess glycosyltransferase
79 and transpeptidase activity, whereas class B PBPs only contain a transpeptidase domain
80 (Höltje, 1998, Sauvage et al., 2008, Goffin and Ghuysen, 1998). In addition, some species
81 such as *Escherichia coli*, *Staphylococcus aureus* and *Streptococcus pneumoniae* encode
82 monofunctional glycosyltransferases (MGTs) that can also incorporate lipid II into the
83 growing glycan strand (Park and Matsuhashi, 1984, Park et al., 1985, Karinou et al., 2018,
84 Wang et al., 2001, Hara and Suzuki, 1984).

85 *B. subtilis* encodes four class A PBPs and no MGT, however, deletion of all class A PBPs
86 only manifests in small PG changes (McPherson and Popham, 2003). Recently, it has been
87 shown that members of the SEDS (shape, elongation, division, sporulation) family of
88 proteins, namely RodA and FtsW, also act as glycosyltransferases (Meeske et al., 2016, Cho
89 et al., 2016, Emami et al., 2017, Taguchi et al., 2019). Both, RodA and FtsW, form

90 complexes with cognate class B PBPs to enable polymerization and crosslinking of glycan
91 strands (Cho et al., 2016, Taguchi et al., 2019, Leclercq et al., 2017, Fraipont et al., 2011,
92 Reichmann et al., 2019). Interestingly, SEDS proteins and the class B PBPs are more
93 conserved among different bacterial species than class A PBPs (Meeske et al., 2016).
94 In rod-shaped bacteria, peptidoglycan is synthesized by two multiprotein complexes, the
95 elongasome that is essential for the cell elongation and the divisome that is crucial for the
96 formation of the division septum (Nanninga, 1991, Carballido-Lopez and Formstone, 2007,
97 Typas et al., 2012, Errington and Wu, 2017). RodA is part of the elongasome and is essential
98 in many bacteria including *B. subtilis* and *S. pneumoniae* (Liu et al., 2017, Henriques et al.,
99 1998). Depletion of RodA results in the production of enlarged, spherical cells in *B. subtilis*
100 (Henriques et al., 1998). In contrast, FtsW is essential for cell division and cells depleted for
101 FtsW grow as long filaments (Kobayashi et al., 2003, Boyle et al., 1997, Gamba et al., 2016).
102 *B. subtilis* harbors a sporulation specific member of the SEDS family, SpoVE in addition to
103 RodA and FtsW. SpoVE is dispensable for growth, however, it is essential for the synthesis
104 of the spore cortex peptidoglycan (Henriques et al., 1992, Ikeda et al., 1989). Other *Bacillus*
105 species such as *B. cereus* and *B. anthracis* possess 4 to 5 FtsW/RodA proteins and strains of
106 different serotypes of the human pathogen *Listeria monocytogenes* encode even up to 6
107 FtsW/RodA homologs in their genome. However, their functions have not yet been
108 investigated.
109 Here, we determined the role of the different FtsW and RodA homologs for the growth and
110 cell morphology of *L. monocytogenes*. Our results show that *L. monocytogenes* encodes two
111 FtsW and three RodA enzymes. Absence of either FtsW1 or of all three RodA proteins is
112 lethal under standard laboratory conditions. *L. monocytogenes* infections are usually treated
113 with high doses of β-lactam antibiotics such as ampicillin, which inhibit the transpeptidase
114 activity of PBPs (Swaminathan and Gerner-Smidt, 2007). We demonstrate that the expression

115 of two SEDS proteins, FtsW2 and RodA3, is induced in the presence of β-lactam antibiotics
116 likely to compensate for the inhibition of PBPs and that a *rodA3* mutant is more sensitive to
117 the β-lactam antibiotic cefuroxime. Antimicrobials inhibiting the activity of proteins of the
118 SEDS family could therefore potentially improve the treatment of *Listeria* infections in the
119 future.
120

121 **Materials and Methods**

122 **Bacterial strains and growth conditions**

123 All strains and plasmids used in this study are listed in Table S1. Strain and plasmid
124 constructions are described in the supplemental materials and method section and all primers
125 used in this study are listed in Table S2. *E. coli* strains were grown in Luria-Bertani (LB)
126 medium and *L. monocytogenes* strains in brain heart infusion (BHI) medium at 37°C unless
127 otherwise stated. If necessary, antibiotics and supplements were added to the medium at the
128 following concentrations: for *E. coli* cultures, ampicillin (Amp) at 100 µg/ml and kanamycin
129 (Kan) at 30 µg/ml, and for *L. monocytogenes* cultures, chloramphenicol (Cam) at 10 µg/ml,
130 kanamycin (Kan) at 30 µg/ml and isopropyl β-D-1-thiogalactopyranoside (IPTG) at 1 mM.
131 We used the *L. monocytogenes* strain 10403S and derivatives thereof. However, we refer to
132 *L. monocytogenes* EGD-e gene and locus tag numbers as this was the first fully sequenced *L.*
133 *monocytogenes* strain.
134

135 **Growth curves**

136 Overnight cultures of wildtype *L. monocytogenes* 10403S and the indicated deletion strains
137 were diluted to an OD_{600} of 0.01 or 0.05 in 15 ml BHI medium and the cultures were
138 incubated at 37°C with shaking. Growth was monitored by determining OD_{600} readings at
139 hourly intervals. For growth curves with the IPTG-inducible depletion strains 10403SΔ*ftsW1*
140 i*ftsW* (ANG4314), 10403SΔ*ftsW1* i*ftsW2* (ANG5119) and 10403SΔ*rodA1-3* i*rodA1*

141 (ANG5192), the strains were cultivated overnight in the presence of 1 mM IPTG. The next
142 day, cells were washed once with fresh medium, diluted 1:50 in 5 ml BHI medium and grown
143 for 8-10 h in the absence of the inducer. The cultures were diluted 1:100 into fresh BHI
144 medium and grown until the next morning at 37°C. The depleted cells were then diluted to an
145 OD_{600} of 0.01 and grown in the presence or absence of 1 mM IPTG at 37°C. Averages and
146 standard deviations from three independent experiments were plotted.
147

148 **RNA extraction and quantitative real-time PCR (qRT-PCR)**

149 For the extraction of RNA from *rodA* complementation strains, overnight cultures of *L.*
150 *monocytogenes* strains 10403S, 10403SΔ*rodA1*Δ*rodA3*, 10403SΔ*rodA1*Δ*rodA3* pIMK3-
151 *rodA1,* 10403SΔ*rodA1*Δ*rodA3* pIMK3-*rodA2* and 10403SΔ*rodA1*Δ*rodA3* pIMK3-*rodA3*
152 were diluted in BHI medium (with 1 mM IPTG for the plasmid-containing complementation
153 strains) to an OD_{600} of 0.05 and incubated at 37°C until the cultures reached an OD_{600} of 1.
154 For the extraction of RNA from strain 10403SΔ*rodA1-3* i*rodA1* (ANG5192), bacteria were
155 grown as described for the growth curve assay to deplete RodA1. Next, 10403S and depleted
156 cells of 10403SΔ*rodA1-3* i*rodA1* were diluted to an OD_{600} of 0.01 and grown in BHI medium
157 in the presence or absence of IPTG until an OD_{600} of 0.5. Twenty mls of the cultures were
158 mixed with 47 ml guanidine thiocyanate (GTC) buffer (5 M GTC, 0.5% N-lauryl sarcosine,
159 0.1 M β-mercaptoethanol, 0.5% Tween-80, 10 mM Tris-HCl pH 7.5), bacteria were harvested
160 by centrifugation and subsequently lysed using the FastRNA™ Pro Blue kit (MP
161 Biomedicals). The total RNA was isolated by chloroform extraction and ethanol precipitation
162 and further purified using the RNeasy mini kit (Qiagen) and finally treated with TURBO
163 DNase (Invitrogen). cDNA was synthesized from 10 ng of RNA using the Superscript III first
164 strand synthesis kit (Invitrogen). The expression of *rodA1*, *rodA2* and *rodA3* in the different
165 strains was assessed using the TaqMan® probe-based gene expression assay (Applied

166 Biosystems). Expression of *gyrB* was used as control. The cycle threshold (Ct) values
167 obtained for *rodA1*, *rodA2* and *rodA3* were normalized to the values obtained for *gyrB*. The
168 fold changes of gene expression for the different strains were calculated using the ΔΔCt
169 method.
170
171 **Determination of minimal inhibitory concentration (MIC)**
172 The minimal inhibitory concentration for bacitracin, penicillin and moenomycin and
173 lysozyme was determined using a microbroth dilution assay in 96-well plates. Approximately
174 10^4 *L. monocytogenes* cells were used to inoculate 200 µl BHI containing two-fold dilutions
175 of the different antimicrobials. The starting antibiotic concentrations were: 1 mg/ml for
176 bacitracin A, 1 µg/ml for penicillin G, 0.8 or 1.6 µg/ml for moenomycin, 8 µg/ml cefuroxime
177 and 10 mg/ml for lysozyme. The OD_{600} readings were determined after incubating the 96-
178 well plates for 24 h at 37°C with shaking at 500 rpm in a plate incubator (Thermostar, BMG
179 Labtech). The MIC value refers to the antibiotic concentration at which bacterial growth was
180 inhibited by >90%.
181
182 **Determination of antibiotic susceptibility using a spot plating assay**
183 Overnight cultures of the indicated *L. monocytogenes* strains were adjusted to an OD_{600} of 1
184 and 5 µl of serial dilutions were spotted on BHI agar plates or BHI agar plates containing 1
185 µg/ml cefuroxime and where indicated also 1 mM IPTG. Plates were photographed after
186 incubation at 37°C for 24 h.
187
188 **Fluorescence and phase contrast microscopy**
189 For bacterial cell length measurements, 100 µl of mid-log cultures were mixed with 5 µl of
190 100 µg/ml nile red solution to stain the cell membrane. Following incubation at 37°C for 20

191 min, the cells were washed once with PBS and resuspended in 50 µl PBS. 1.5 µl of the
192 different samples were spotted on microscope slides covered with a thin agarose film (1.5 %
193 agarose in distilled water), air-dried and covered with a cover slip. Phase contrast and
194 fluorescence images were taken using a Zeiss Axio Imager.A1 microscope coupled to a
195 AxioCam MRm and a 100x objective and processed using the Zen 2012 software (blue
196 edition). For the detection of nile red fluorescence signals, the Zeiss filter set 00 was used.
197 For the cell length determinations, 300 cells were measured for each experiment and the
198 median cell length was calculated. Averages and standard deviations of the median cell
199 length of three independent experiments were plotted.
200
201 **Peptidoglycan isolation and analysis**
202 Overnight cultures of *L. monocytogenes* 10403S, 10403SΔ*rodA1*Δ*rodA3* and
203 10403SΔ*rodA1*Δ*rodA3* pIMK3-*rodA1* were used to inoculate 1 L BHI broth (with 1 mM
204 IPTG for the complementation strain 10403SΔ*rodA1*Δ*rodA3* pIMK3-*rodA1*) to a starting
205 OD_{600} of 0.06. The cultures were grown at 37°C until they reached an OD_{600} of 1, at which
206 point the cultures were cooled on ice for 1 h. The bacteria were subsequently collected by
207 centrifugation and peptidoglycan was purified and digested with mutanolysin as described
208 previously (de Jonge et al., 1992, Corrigan et al., 2011). Digested muropeptides were
209 analyzed by high-performance liquid chromatography (HPLC) and recorded at an absorption
210 of 205 nm as described previously (de Jonge et al., 1992). For quantification, the areas of the
211 main muropeptide peaks were integrated using the Agilent Technology ChemStation
212 software. The sum of the peak areas was set to 100% and individual peak areas were
213 determined. Averages and standard deviations from three independent extractions were
214 calculated.
215

216 **β-galactosidase assay**

217 For the determination of the β-galactosidase activity, overnight cultures of strains 10403S
218 pPL3e-$P_{lmo2689}$-*lacZ*, 10403SΔ*rodA1* pPL3e-$P_{lmo2689}$-*lacZ* and 10403SΔ*rodA1*Δ*rodA2* pPL3e-
219 $P_{lmo2689}$-*lacZ* were diluted 1:100 in fresh BHI medium and grown for 6 h at 37°C. Sample
220 collection and preparation were performed as described previously (Gründling et al., 2004).
221 Briefly, OD_{600} readings were determined (for the final β-galactosidase unit calculations) for
222 the different cultures after 6 h of growth and cells from 1 ml culture were pelleted by
223 centrifugation for 10 min at 13,200 x g, resuspended in 100 µl ABT buffer (60 mM K_2HPO_4,
224 40 mM KH_2PO_4, 100 mM NaCl, 0.1% Triton X-100, pH 7.0), snap frozen in liquid nitrogen
225 and stored at -80°C until use. For the identification of substances inducing the expression of
226 the *lmo2689-lmo2686* operon, an overnight culture of strain 10403S pPL3e-$P_{lmo2689}$-*lacZ* was
227 diluted 1:100 in fresh BHI medium and the culture incubated with shaking at 37°C until an
228 OD_{600} of 0.5-0.6. The culture was divided into several flasks and incubated for two hours at
229 37°C in the presence or absence of the following substances: 0.5 µg/ml ampicillin, 0.05
230 µg/ml penicillin, 0.5 µg/ml vancomycin, 4 µg/ml cefuroxime, 0.05 µg/ml moenomycin, 0.5
231 mg/ml lysozyme, 1% ethanol, 300 µg/ml $MgSO_4$ or 300 µg/ml EDTA. Bacteria were pelleted
232 and samples frozen as described above.

233 Samples were thawed and 1:10 dilutions were prepared in ABT buffer. Fifty µl of the 1:10
234 diluted samples were mixed with 10 µl of 0.4 mg/ml 4-methyl-umbelliferyl-β-D-
235 galactopyranoside (MUG) substrate prepared in DMSO and incubated for 60 min at room
236 temperature (RT). A reaction with ABT buffer alone was used as negative control. Following
237 this incubation step, 20 µl of each reaction was diluted into 180 µl of ABT buffer in a black
238 96-well plate and fluorescence values were measured using an HIDEX Sense Microplate
239 Reader at 355 nm excitation and 460 nm emission wavelengths. 0.125-20 µM of the
240 fluorescent 4-methylumbelliferone (MU) standard were used to obtain a standard curve. β-

241 galactosidase units were calculated as (pmol of substrate hydrolyzed x dilution factor)/(ml
242 culture volume x OD_{600} x minute). The amount of hydrolyzed substrate was determined from
243 the standard curve as (emission reading – y intercept)/slope.
244
245 **Bacterial two-hybrid assays**
246 Protein-protein interactions between the different FtsW/RodA homologs and class B PBPs
247 were analyzed using the bacterial adenylate cyclase two-hybrid (BACTH) assay (Karimova et
248 al., 1998). The indicated pUT18/pUT18c and pKT25 derivatives were co-transformed into *E.*
249 *coli* strain BTH101. Transformants were selected on LB agar plates containing 100 µg/ml
250 ampicillin, 30 µg/ml kanamycin, 0.1 mM IPTG and 50 µg/ml X-Gal. Images were taken after
251 incubation for 24 h and 48 h at 30°C.
252
253 **Results**
254 ***L. monocytogenes* 10403S encodes six FtsW/RodA homologs**
255 So far, FtsW and RodA proteins of the human pathogen *L. monocytogenes* have not been
256 studied. FtsW and RodA are members of the SEDS (shape, elongation, division, sporulation)
257 family of proteins and are multispanning membrane proteins with 8-10 transmembrane
258 helices and a large extracellular loop (Fig. 1A). Using BLAST, six proteins with homology to
259 the *B. subtilis* FtsW and RodA proteins could be identified in the genome of *L.*
260 *monocytogenes* 10403S (Table 1). The protein encoded by *lmo0421* has the weakest
261 homology to *B. subtilis* FtsW and RodA (Fig. S1, Table 1). *lmo0421* is part of the *sigC*
262 operon, which is comprised of *lmo0422* encoding the PadR-like repressor LstR and *lmo0423*
263 coding for the ECF-type sigma factor SigC (Fig. 1B). The *sigC* operon acts as a lineage II
264 specific heat shock system (Zhang et al., 2005) and is therefore not encoded in all *L.*

265 *monocytogenes* genomes. Due to the weak homology to FtsW and RodA and its absence in *L.*
266 *monocytogenes* strains of lineage I and III, Lmo0421 was excluded from further analysis.
267 The *L. monocytogenes* protein Lmo1071 is the closest homolog to *B. subtilis* FtsW with a
268 sequence identity of 48% (Table 1). Furthermore, *L. monocytogenes lmo1071* and *B. subtilis*
269 *ftsW* are found in the same chromosomal context. More specifically, *lmo1071* is located
270 between genes *lmo1070*, which encodes a protein with homology to the *B. subtilis* YlaN
271 protein, and *pycA* coding for the pyruvate carboxylase, which are also adjacent to *ftsW* in *B.*
272 *subtilis*. This analysis suggests that gene *lmo1071* encodes the cell division protein FtsW.
273 However, *L. monocytogenes* encodes a second protein, Lmo2688, that shares a higher degree
274 of homology to the *B. subtilis* FtsW as compared to the *B. subtilis* RodA protein (Table 1).
275 Due to these similarities and additional data presented in this study, we refer to Lmo1071 and
276 Lmo2688 as FtsW1 and FtsW2, respectively.
277 The BLAST search with the *B. subtilis* RodA sequence as a query sequence yielded the *L.*
278 *monocytogenes* protein Lmo2428 as the closest homolog with a sequence identity of 40%
279 (Table 1). In addition to Lmo2428, two additional RodA homologs are present in *L.*
280 *monocytogenes*, namely Lmo2427 and Lmo2687. As presented below, Lmo2427, Lmo2428
281 and Lmo2687 are likely bona-fide RodA homologs and were therefore renamed RodA1,
282 RodA2 and RodA3, respectively. *rodA1* is located adjacent to *rodA2*, but despite their
283 proximity, *rodA1* and *rodA2* are likely not transcribed as part of the same operon (Toledo-
284 Arana et al., 2009). In contrast, *rodA3* and *ftsW2* are part of the four-gene operon *lmo2689-*
285 *lmo2686*. Lmo2689 is similar to a Mg^{2+}-type ATPase, whereas *lmo2686* encodes a protein of
286 unknown function. Analysis of around 2000 genomes of *L. monocytogenes* strains presently
287 available at NCBI revealed that the five FtsW/RodA homologs named here FtsW1, FtsW2,
288 RodA1, RodA2 and RodA3 are conserved in the different strains with one exception; *L.*
289 *monocytogenes* 4b strains of the sequence type ST2 lack homologs of RodA3 and FtsW2.

290

291 ***lmo1071* encodes FtsW1 and is essential for the survival of *L. monocytogenes***

292 The cell division protein FtsW is essential for growth in the Gram-negative and Gram-
293 positive model organisms *E. coli* and *B. subtilis* (Boyle et al., 1997, Ikeda et al., 1989,
294 Khattar et al., 1994, Kobayashi et al., 2003). Depletion of FtsW in these organisms leads to a
295 block in cell division and formation of elongated cells (Boyle et al., 1997, Gamba et al.,
296 2016). All our attempts to delete the *ftsW1* gene in *L. monocytogenes* 10403S remained
297 unsuccessful, suggesting that FtsW1 is also essential for growth in *Listeria*. Next, strain
298 10403SΔ*ftsW1* i*ftsW1* was constructed, in which the expression of *ftsW1* is controlled by an
299 IPTG-inducible promoter. While no difference in the growth was observed between the
300 wildtype and FtsW1-depletion strain (likely due to leakiness of the inducible promoter) (Fig.
301 2A), cells depleted for FtsW1 were significantly elongated (Fig. 2B-C). Bacteria depleted for
302 FtsW1 had a median cell length of 3.41±0.16 µm, while wildtype and 10403SΔ*ftsW1* i*ftsW1*
303 bacteria grown in the presence of 1 mM IPTG had a median cell length of 1.85±0.16 µm and
304 1.93±0.07 µm, respectively (Fig. 2C). These data indicate that *lmo1071* encodes the cell
305 division specific SEDS protein FtsW.

306

307 ***L. monocytogenes* encodes a second FtsW protein**

308 To our knowledge, all bacteria analyzed to date possess only one FtsW protein that is
309 essential for cell survival. We identified a second potential FtsW protein, Lmo2688, in *L.*
310 *monocytogenes*. In contrast to *ftsW1,* a *L. monocytogenes ftsW2* deletion strain could be
311 constructed and no significant growth or cell morphology phenotypes could be observed for
312 the Δ*ftsW2* deletion strain (Fig. S2). In a previous study, it was reported that the operon
313 comprised of genes *lmo2689-lmo2686* is only minimally expressed when *L. monocytogenes*
314 10403S is grown in BHI broth (Lobel and Herskovits, 2016). We reasoned that if *ftsW2* does

315 indeed code for a second FtsW protein, it should be possible to delete *ftsW1* in a strain in
316 which *ftsW2* is artificially expressed from an IPTG-inducible promoter. Indeed, strain
317 10403SΔ*ftsW1* i*ftsW2* could be generated in the presence of IPTG. In contrast, we were
318 unable to generate strain 10403SΔ*ftsW1* when any of the other FtsW/RodA homologs
319 Lmo2427 (RodA1), Lmo2428 (RodA2) or Lmo2687 (RodA3) were expressed from the same
320 IPTG-inducible promoter system. While prolonged depletion of FtsW2 in strain
321 10403SΔ*ftsW1* i*ftsW2* had again no impact on the growth, the cells were significantly
322 elongated in the absence of the inducer compared to wildtype or bacteria grown in the
323 presence of inducer (Fig. 3). These data strongly suggest that *ftsW2* encodes a second FtsW
324 enzyme while the remaining three proteins Lmo2427, Lmo2428 and Lmo2687 likely function
325 as RodA proteins.
326
327 ***L. monocytogenes* encodes three RodA homologs**
328 We were able to assign roles for two of the FtsW/RodA homologs as FtsW-like proteins.
329 However, *L. monocytogenes* encodes three additional homologs, which show a higher
330 similarity to the *B. subtilis* RodA protein as compared to the *B. subtilis* FtsW protein (Table
331 1). As described above, expression of none of the enzymes Lmo2427, Lmo2428 or Lmo2687
332 was able to rescue the growth of an *ftsW1* deletion strain, indicating that these enzymes likely
333 function as RodA proteins in *L. monocytogenes* and hence they were renamed RodA1,
334 RodA2 and RodA3, respectively. All attempts to construct a *rodA1-3* triple mutant failed
335 further corroborating that these proteins function as RodA proteins and at least one of them
336 needs to be present for cell viability. To determine whether the different RodA homologs
337 have distinct functions or whether they are merely duplications, single and double mutant
338 strains were generated. No significant differences with regards to growth and cell length
339 could be observed between the wildtype strain 10403S and single *rodA1*, *rodA2* or *rodA3*

340 deletion strains (Fig. S3). Similar observations were made with the *rodA* double mutant
341 strains 10403SΔ*rodA1*Δ*rodA2* and 10403SΔ*rodA2*Δ*rodA3* (Fig. 4). However, cells lacking
342 RodA1 and RodA3 were shorter (1.3±0.03 µm) compared to wildtype cells (1.9±0.06 µm,
343 Fig. 4B-C), indicating that either RodA1 or RodA3 needs to be present for *L. monocytogenes*
344 to maintain its rod shape. RodA3 is part of the *lmo2689-lmo2686* operon that is only
345 minimally expressed when *L. monocytogenes* is grown in BHI broth (Lobel and Herskovits,
346 2016). The fact that we observe differences in cell morphology between a *rodA1* single and
347 the *rodA1/rodA3* double mutant, suggests that the function of the two proteins could be
348 additive or that *rodA3* expression, which is only minimally expressed in a wildtype strain
349 under standard laboratory growth conditions, might increase upon deletion of *rodA1*. To test
350 if *rodA3* expression is increased in the absence of other RodA proteins, we fused the
351 promoter upstream of *lmo2689* and driving *rodA3* expression to *lacZ* and inserted this fusion
352 into the chromosome of wildtype 10403S, the *rodA1* and the *rodA1/rodA2* deletion strains.
353 The promoter activity was indeed 1.5- to 2-fold higher in the *rodA1* and *rodA1/rodA2* mutant
354 strains as compared to the wildtype, as assessed by the increase in the β-galactosidase activity
355 (Fig. 4G). This result indicates that expression of the *lmo2689-lmo2686* operon, which
356 encodes FtsW2 and RodA3, is induced in the absence of RodA1, suggesting a coordination of
357 the expression of the different RodA homologs.
358 To confirm that the decrease in cell length of the double mutant strain 10403SΔ*rodA1*Δ*rodA3*
359 depends on the absence of RodA1 and RodA3, complementation strains with IPTG-inducible
360 expression of *rodA1* or *rodA3* were constructed. Expression of RodA1 restored the cell length
361 to 1.84±0.1 µm, which is comparable to the cell length of wildtype cells (1.76±0.15 µm, Fig.
362 4E). On the other hand, expression of *rodA3* from an ectopic locus and IPTG-inducible
363 promoter in strain 10403SΔ*rodA1*Δ*rodA3* led to the formation of longer cells with an average
364 cell length of 2.47±0.01 µm (Fig. 4D-E). These results indicate that induction of RodA3 from

365 the IPTG-inducible promoter likely results in an overproduction of the protein as compared to
366 the expression from the native promoter. To confirm that *rodA3* expression is increased when
367 expressed from the IPTG-inducible promoter as compared to its native promoter, *rodA3*
368 transcript levels were assessed by qRT-PCR in the wildtype strain, the
369 10403SΔ*rodA1*Δ*rodA3* deletion strain and strain 10403SΔ*rodA1*Δ*rodA3* i*rodA3* grown in the
370 presence of IPTG (Fig. 4H). Significant higher *rodA3* transcript levels were detected in the
371 inducible strain in the presence of IPTG as compared to the wildtype strain. Similarly,
372 expression of *rodA3* from an IPTG-inducible promoter in wildtype 10403S led to the
373 formation of elongated cells with an average cell length of 2.49±0.08 µm, whereas additional
374 expression of *rodA1* or *rodA2* using the same inducible system had no impact on the cell
375 length of 10403S (Fig. S4). These results highlight that in particular fine-tuning of RodA3
376 production is essential for cell-length determination in *L. monocytogenes*.
377 The observation that the *rodA1*/*rodA3* double mutant forms shorter cells suggests that RodA2
378 is not sufficient to maintain the cell length of *L. monocytogenes*. There are several possible
379 explanations for this: RodA2 might have a reduced activity as compared to RodA1 or RodA3.
380 RodA2 might have a function that is different from RodA1 and RodA3 or the protein levels
381 of RodA2 might be sufficient to maintain cell viability but too low to maintain the rod shape.
382 To investigate this further, a strain was constructed which lacks *rodA1* and *rodA3*, but carries
383 pIMK3-*rodA2* to allow for IPTG-inducible expression of *rodA2* in addition to the expression
384 of *rodA2* from its native locus (10403SΔ*rodA1*Δ*rodA3* i*rodA2*). In the absence of the inducer,
385 the cells had a median cell length of 1.2±0.03 µm (data not shown). However, the cell length
386 of strain 10403SΔ*rodA1*Δ*rodA3* i*rodA2* increased to 1.71±0.8 µm when the strain was grown
387 in the presence of IPTG (Fig. 4F). Therefore, additional expression of *rodA2*, which was
388 verified by qRT-PCR (Fig. 4I), can partially complement the cell length phenotype of the
389 *rodA1*/*rodA3* deletion strain, suggesting that RodA2 has a similar function as RodA1 and

390 RodA3, but that it has either a lower activity or is not expressed in sufficient amounts from
391 its native promoter for proper cell length maintenance.
392 As stated above, several attempts to construct a strain inactivated for all three RodA
393 homologs remained unsuccessful, suggesting that at least one of the proteins RodA1, RodA2
394 or RodA3 needs to be present for the viability of *L. monocytogenes*. The results presented so
395 far indicate that RodA1 is the most important RodA homolog considering that RodA2 alone
396 is not sufficient to maintain the rod shape and that RodA3 is only minimally expressed under
397 standard laboratory conditions (Lobel and Herskovits, 2016) and also lacking in *L.*
398 *monocytogenes* 4b strains of the sequence type ST2. To understand the impact of RodA
399 enzymes on cell growth and cell division in *L. monocytogenes*, a strain was constructed
400 which lacks all three *rodA* genes from its genome, but harbors pIMK3-*rodA1* to enable IPTG-
401 inducible expression of RodA1. Prolonged depletion of RodA1 in strain 10403SΔ*rodA1-3*
402 i*rodA1* led to a growth defect that was not seen when the strain was grown in the presence of
403 the inducer (Fig. 5A). However, the depletion was not efficient enough to see a complete
404 growth inhibition, which would be expected for a strain lacking all three RodA homologs.
405 This is likely caused by residual *rodA1* expression from the inducible promoter even in the
406 absence of IPTG. Consistent with this notion, even after prolonged depletion, *rodA1*
407 transcripts could still be detected in strain 10403SΔ*rodA1-3* i*rodA1* as assessed by qRT-PCR
408 (Fig. S5). However, cells of the *L. monocytogenes* strain 10403SΔ*rodA1-3* i*rodA1* that were
409 grown without IPTG were significantly shorter with a cell length of 1.18±0.08 µm as
410 compared to cells of the double mutant 10403SΔ*rodA1*Δ*rodA3* or the wildtype strain 10403S
411 (Fig. 5B, D). Interestingly, different cell morphologies could be observed for strain
412 10403SΔ*rodA1-3* i*rodA1* after prolonged RodA1 depletion (Fig. 5C). The placement of the
413 division septum was affected in some cells and daughter cells of different size or cells with
414 two septa were observed (Fig. 5C). These morphological defects could be complemented, and

415 the cell length increased to 1.95±0.04 µm upon addition of IPTG and expression of RodA1
416 (Fig. 5D). These data highlight that RodA1 alone is sufficient to maintain the cell shape of *L.*
417 *monocytogenes*.
418
419 **Decreased moenomycin and lysozyme resistance in the absence of RodA homologs**
420 Next, we wondered whether the absence of FtsW or RodA proteins affects the resistance of *L.*
421 *monocytogenes* towards the antibiotics penicillin, bacitracin and moenomycin, which target
422 different steps in the peptidoglycan biosynthesis process. Penicillin binds to the
423 transpeptidase domain of PBPs and inhibits their function, leading to a reduced crosslinking
424 of the peptidoglycan (Nakagawa et al., 1979, Korsak et al., 2010). Bacitracin inhibits the
425 dephosphorylation of the bactoprenol carrier leading to a block in lipid II synthesis (Stone
426 and Strominger, 1971). The phosphoglycolipid antibiotic moenomycin inhibits the
427 glycosyltransferase activity of bifunctional PBPs and thereby prevents the polymerization of
428 the glycan chain (van Heijenoort et al., 1987).
429 No significant differences could be observed in terms of resistance against penicillin,
430 bacitracin or moenomycin for the FtsW1 depletion strain 10403SΔ*ftsW1* i*ftsW1*. This is
431 presumably due to basal level expression of *ftsW1* even in the absence of the inducer.
432 Simultaneous deletion of *rodA1* and *rodA3* resulted in a slight decrease in the MIC for
433 penicillin, however, this difference was not significant (Fig. 6A). On the other hand, strain
434 10403SΔ*rodA1*Δ*rodA3* was 2-4-fold more sensitive to the antibiotic bacitracin (Fig. 6B). This
435 phenotype could be complemented by expressing either RodA1, RodA2 or RodA3 from an
436 IPTG-inducible promoter (Fig. 6B).
437 As described above, moenomycin inhibits the transglycosylase activity of PBPs leading to a
438 decreased activity of these enzymes. In the absence of RodA1 and RodA3, cells are more
439 susceptible to a reduced activity of PBPs manifesting in a 4-fold reduced resistance to

440 moenomycin (Fig 6C). Induction of RodA1 expression in strain 10403SΔ*rodA1*Δ*rodA3*
441 resulted in a significantly higher resistance to moenomycin as compared to the wildtype
442 strain 10403S and expression of RodA2 or RodA3, led to partial or complete
443 complementation of the moenomycin sensitivity (Fig. 6C).
444 Moreover, resistance to lysozyme, an enzyme that cleaves the linkage between N-acetyl
445 muramic acid and N-acetylglucosamine residues of the peptidoglycan, was drastically
446 decreased in strain 10403SΔ*rodA1*Δ*rodA3* and could be fully restored by expression of
447 RodA1, RodA2 or RodA3 (Fig. 6D). Lysozyme resistance in *L. monocytogenes* is mainly
448 accomplished by two modifications of the peptidoglycan; deacetylation of N-
449 acetylglucosamine residues by PgdA or O-acetylation of N-acetylmuramic acid residues by
450 OatA (Boneca et al., 2007, Aubry et al., 2011). To determine whether the activity of PgdA is
451 changed in the absence of RodA1 and RodA3, peptidoglycan was purified from the
452 10403SΔ*rodA1*Δ*rodA3* mutant strain, digested with mutanolysin and the resulting
453 muropeptides analyzed by HPLC. Peptidoglycan samples isolated from the wildtype strain
454 10403S and the complementation strain 10403SΔ*rodA1*Δ*rodA3* i*rodA1*, that had been grown
455 in the presence of IPTG, were analyzed as controls (Fig. 6E). The main muropeptide peaks
456 were assigned as described previously (Rismondo et al., 2015, Burke et al., 2014). Peaks 1
457 and 2 correspond to the acetylated and deacetylated monomeric muropeptides, respectively,
458 whereas peak 3 and peaks 4-6 are acetylated and deacetylated muropeptide dimers,
459 respectively. Deletion of *rodA1* and *rodA3* led to a reduction of both monomeric
460 muropeptides and therefore to an increase in crosslinked peptidoglycan fragments by
461 approximately 2% as compared to the wildtype strain 10403S, in which 65% of the
462 peptidoglycan was cross-linked (Fig. 6F). However, no significant difference with regards to
463 the deacetylated muropeptides could be observed between wildtype 10403S, strain
464 10403SΔ*rodA1*Δ*rodA3* and the 10403SΔ*rodA1*Δ*rodA3* i*rodA1* complementation strain (Fig.

465 6F). These results suggest that the lysozyme sensitivity phenotype of strain
466 10403SΔ*rodA1*Δ*rodA3* is not caused by changes in the peptidoglycan deacetylation, but
467 rather due to general defects in the peptidoglycan structure.
468
469 **Cell wall-acting antibiotics induce the promoter of *lmo2689***
470 The operon *lmo2689-lmo2686*, that contains the genes encoding FtsW2 and RodA3, is only
471 minimally expressed under standard laboratory conditions (Lobel and Herskovits, 2016). A
472 genome-wide transcriptional analysis performed in *L. monocytogenes* strain LO28 has shown
473 that *lmo2687, lmo2688* and *lmo2689* are part of the CesR regulon (Nielsen et al., 2012). The
474 cephalosporin sensitivity response regulator CesR is part of the CesRK two-component
475 system that regulates the transcription of several cell envelope-related genes in response to
476 changes in cell wall integrity, such as caused by the presence of cell wall-acting antibiotics or
477 alcohols including ethanol (Gottschalk et al., 2008, Kallipolitis et al., 2003, Nielsen et al.,
478 2012). Therefore, we next used the *lmo2689* promoter-*lacZ* fusion described above, to assess
479 if expression of the *lmo2689-lmo2686* operon is induced in the presence of antibiotics that
480 target different processes of the PG biosynthesis or ethanol. Indeed, increased β-galactosidase
481 activity could be measured for cells that had been grown in the presence of sub-inhibitory
482 concentrations of the β-lactam antibiotics ampicillin, penicillin and cefuroxime and the
483 phosphoglycolipid moenomycin (Fig. 7A). In contrast, no increase in β-galactosidase activity
484 could be detected upon addition of vancomycin, lysozyme or ethanol as compared to
485 untreated control cells (Fig. 7A). We also tested whether the presence of $MgSO_4$ or EDTA
486 has an impact on the *lmo2689* promoter activity since *lmo2689* encodes a putative Mg^{2+}-type
487 ATPase. However, the β-galactosidase activity of cells grown in the presence of $MgSO_4$ or
488 EDTA was comparable to the β-galactosidase activity seen for untreated cells (Fig. 7A).
489 These results indicate that the expression of *ftsW2* and *rodA3*, that are part of the *lmo2689-*

490 *lmo2686* operon, are induced in the presence of various cell wall-acting antibiotics,
491 suggesting that FtsW2 and RodA3 might be important for the intrinsic resistance of *L.*
492 *monocytogenes* against these antibiotics. However, no significant differences in MICs for
493 penicillin and moenomycin could be observed between wildtype 10403S, the *ftsW2* or *rodA3*
494 single mutant strains or the *ftsW2/rodA3* double mutant (Fig. S6). However, there was a slight
495 reduction in the resistance of the *rodA3* single mutant against cefuroxime as compared to the
496 wildtype (Fig. S6). To further assess whether there is a difference in the cefuroxime
497 resistance between the *L. monocytogenes* wildtype strain 10403S and the *rodA1*, *rodA2* and
498 *rodA3* single mutant strains, dilutions of overnight cultures were spotted on BHI agar plates
499 with or without 1 µg/ml cefuroxime. Deletion of *rodA1* or *rodA2* results in a slightly reduced
500 ability of these strains to grow on BHI plates supplemented with 1 µg/ml cefuroxime as
501 compared to the wildtype 10403S strain (Fig. 7B). However, deletion of *rodA3* leads to a
502 stronger reduction of growth on BHI plates containing 1 µg/ml cefuroxime as compared to
503 the *rodA1* and *rodA2* single mutants (Fig. 7B). Interestingly, overexpression of RodA3, but
504 not of RodA1 or RodA2, also resulted in decreased resistance towards cefuroxime as
505 compared to the wildtype strain 10403S (Fig. 7C). Our results therefore suggest that *L.*
506 *monocytogenes* induces the expression of *rodA3* and *ftsW2* in the presence of β-lactam
507 antibiotics and moenomycin to compensate for the inhibition of the glycosyltransferase and
508 transpeptidase activity of PBPs. In particular RodA3 seems to play an important function for
509 the intrinsic cephalosporine resistance in *L. monocytogenes* and its expression needs to be
510 finely balanced as both its absence as well as increased expression have detrimental effects
511 on resistance against this antibiotic.
512
513 **FtsW and RodA proteins interact with class B PBPs**

514 Previous studies have shown that members of the SEDS protein family act together with a
515 cognate class B PBP to synthesize and crosslink peptidoglycan (Henriques et al., 1998, Wei
516 et al., 2003, Reichmann et al., 2019, Gamba et al., 2009, Daniel et al., 1996). *L.*
517 *monocytogenes* encodes three class B PBPs, namely PBP B1, PBP B2 and PBP B3. To
518 identify potential protein-protein interactions between the *L. monocytogenes* class B PBPs
519 and the FtsW/RodA proteins, a bacterial adenylate cyclase two-hybrid (BACTH) analysis
520 was performed. Interactions were detected between the three *L. monocytogenes* PBP B1, PBP
521 B2 and PBP B3 and all FtsW and RodA homologs (Fig. 8). These results suggest that the
522 FtsW and RodA proteins also form a complex with class B PBPs in *L. monocytogenes*.
523 However, using this bacterial two hybrid approach it was not possible to determine specific
524 SEDS protein and class B PBP pairs.
525
526 **Discussion**
527 Bacterial cell elongation and cell division need to be tightly regulated to maintain the cell
528 shape. This is accomplished by two multiprotein complexes, the elongasome and the
529 divisome, which are coordinated by the actin homolog MreB and the tubulin homolog FtsZ,
530 respectively (Carballido-Lopez and Formstone, 2007, Typas et al., 2012, Jones et al., 2001,
531 Errington and Wu, 2017, den Blaauwen, 2018). The SEDS protein FtsW is part of the
532 divisome and essential for growth as shown for many bacteria including *E. coli, B. subtilis*
533 and *S. aureus* (Boyle et al., 1997, Ikeda et al., 1989, Khattar et al., 1994, Kobayashi et al.,
534 2003, Reichmann et al., 2019). Our experiments suggested that FtsW1 is also essential in *L.*
535 *monocytogenes*, however, a second FtsW protein, FtsW2, can compensate for the loss of
536 FtsW1 if it is expressed from an inducible promoter. FtsW2 is encoded in the *lmo2689-*
537 *lmo2686* operon that appears to be only minimally expressed when *L. monocytogenes* 10403S
538 is grown under standard laboratory conditions (Lobel and Herskovits, 2016). The expression

539 of the *lmo2689-lmo2686* operon is regulated by the two-component system CesRK that is
540 activated by cell envelope stress (Kallipolitis et al., 2003, Gottschalk et al., 2008, Nielsen et
541 al., 2012). Using an *L. monocytogenes* strain carrying a $P_{lmo2689}$-*lacZ* promoter fusion, we
542 could detect increased β-galactosidase activity after incubation with sub-inhibitory
543 concentrations of different β-lactam antibiotics including penicillin, cefuroxime, and
544 moenomycin. However, the expression of the *lmo2689-lmo2686* operon was not induced by
545 other cell wall-targeting antibiotics such as vancomycin or the hydrolase lysozyme. This
546 suggests that inhibition of the glycosyltransferase or transpeptidase activity of PBPs leads to
547 activation of the *lmo2689-lmo2686* operon, and hence, to the expression of *ftsW2* as well as
548 *rodA3*.
549 The rod-shape determining protein RodA is part of the elongation machinery. The data
550 presented in this study suggest that *L. monocytogenes* encodes not one but three RodA
551 proteins and depletion of the three RodA enzymes leads to a decreased cell length (Fig. 5).
552 Simultaneous deletion of *rodA1* and *rodA3* already results in the formation of shorter cells,
553 whereas cells of strains deleted for *rodA1/rodA2* or *rodA2/rodA3* have a cell length that is
554 comparable to the wildtype strain 10403S. Taking into consideration that *rodA3* is only
555 minimally expressed under standard laboratory growth conditions in *L. monocytogenes*
556 10403S (Lobel and Herskovits, 2016), the results presented in this study suggest that *rodA3*
557 expression gets induced upon inactivation of RodA1, since we observed morphological
558 differences between the *rodA1* single and the *rodA1/3* double mutant strains. Indeed, β-
559 galactosidase assays confirmed that deletion of *rodA1* or *rodA1/2* increases the activity of the
560 promoter from which *rodA3* is expressed. The data presented in this study also indicate that
561 RodA1 is the "main" RodA enzyme in *L. monocytogenes* as no significant phenotypic
562 changes with regards to growth and cell division could be observed as long as RodA1 was
563 present. On the other hand, RodA2 was only able to compensate for the loss of RodA1 and

564 RodA3, when overproduced from an inducible promoter. Interestingly, cells of strains
565 10403S and 10403SΔ*rodA1*Δ*rodA3* in which *rodA3* is overexpressed from an ectopic locus
566 have an increased cell length as compared to the wildtype. An explanation for this could be
567 that elevated levels of RodA3 lead to the depletion of proteins needed at the cell division site,
568 resulting in an extended synthesis of PG on the lateral wall. Another possibility could be that
569 RodA3 directly inhibits FtsW1 or displaces FtsW1 at the cell division site, leading to a block
570 in cell division and therefore resulting in the formation of elongated cells.
571 Recent studies have shown that SEDS proteins act as glycosyltransferases (Meeske et al.,
572 2016, Emami et al., 2017). The glycosyltransferase activity of PBPs and MGT can be
573 inhibited by moenomycin, whereas RodA/FtsW enzymes are not affected by moenomycin
574 and are therefore important for moenomycin resistance (Tamura et al., 1980, Emami et al.,
575 2017). In good agreement with the importance of SEDS proteins for the intrinsic
576 moenomycin resistance, deletion of the genes encoding two of the three RodA enzymes,
577 RodA1 and RodA3, resulted in an increased moenomycin sensitivity of *L. monocytogenes*
578 (Fig. 6C).
579 In *B. subtilis*, RodA is in a complex with the class B PBP, PBP 2A (also named PbpH), and
580 these two proteins act together to polymerize and crosslink the glycan strands (Wei et al.,
581 2003, Henriques et al., 1998). Similarly, FtsW and PBP 2B form a subcomplex as part of the
582 divisome (Daniel et al., 1996, Gamba et al., 2009). Recently it was shown that RodA-PBP3
583 and FtsW-PBP1 act as cognate pairs in the coccoid bacterium *S. aureus* (Reichmann et al.,
584 2019). Depletion of all three RodA enzymes in *L. monocytogenes*, RodA1, RodA2 and
585 RodA3, leads to a drastic reduction in cell length (Fig. 5). A similar phenotype was observed
586 for a *L. monocytogenes* strain depleted for the essential class B PBP, PBP B1 (Rismondo et
587 al., 2015). In contrast, the absence of either FtsW1 (Fig. 2) or the class B PBP, PBP B2, in *L.*
588 *monocytogenes* results in the formation of elongated cells (Rismondo et al., 2015). These

589 observations suggest that RodA and FtsW might work in a complex with the cognate PBPs
590 PBP B1 and PBP B2 during cell elongation and cell division, respectively. Indeed, protein-
591 protein interactions between FtsW1 and FtsW2 with PBP B2 and between RodA1, RodA2
592 and RodA3 with the PBP B1 could be observed (Fig. 8). However, interactions were also
593 detected between the FtsW proteins and PBP B1 and PBP B3 as well as between the RodA
594 proteins and PBP B2 and PBP B3 (Fig. 8). While these data provide the first line of evidence
595 that SEDS proteins and class B PBPs also form complexes in *L. monocytogenes,* additional
596 work is necessary to determine if specific SEDS-bPBP pairs are formed in *L. monocytogenes*.
597 Taken together, *L. monocytogenes* has a repertoire of PBPs and multiple members of the
598 SEDS family of proteins to produce its rigid cell wall. The expression and the activity of
599 these enzymes need to be tightly regulated in *L. monocytogenes* to maintain its cell shape.
600 Our results suggest that *L. monocytogenes* adapts the expression of a second set of
601 FtsW/RodA enzymes, FtsW2 and RodA3, to environmental stresses such as the presence of
602 β-lactam antibiotics, thereby preventing defects in the peptidoglycan synthesis and
603 subsequent cell lysis. In *L. monocytogenes* strains that lack this back-up system, RodA2
604 might in part fulfil a similar role.
605
606 **Acknowledgements**
607 This work was funded by the Wellcome Trust grants 100289/Z/12/Z and 210671/Z/18/Z to
608 AG and the German research foundation (DFG) grants RI 2920/1-1 to JR and HA6830/1-1 to
609 SH.
610
611

612 **References**
613

614 AUBRY, C., GOULARD, C., NAHORI, M. A., CAYET, N., DECALF, J., SACHSE, M., BONECA, I. G.,
615 COSSART, P. & DUSSURGET, O. 2011. OatA, a peptidoglycan O-acetyltransferase
616 involved in *Listeria monocytogenes* immune escape, is critical for virulence. *J Infect*
617 *Dis,* 204**,** 731-40.
618 BLUMBERG, P. M. & STROMINGER, J. L. 1974. Interaction of penicillin with the bacterial cell:
619 penicillin-binding proteins and penicillin-sensitive enzymes. *Bacteriol Rev,* 38**,** 291-
620 335.
621 BONECA, I. G., DUSSURGET, O., CABANES, D., NAHORI, M. A., SOUSA, S., LECUIT, M.,
622 PSYLINAKIS, E., BOURIOTIS, V., HUGOT, J. P., GIOVANNINI, M., COYLE, A., BERTIN, J.,
623 NAMANE, A., ROUSSELLE, J. C., CAYET, N., PREVOST, M. C., BALLOY, V., CHIGNARD,
624 M., PHILPOTT, D. J., COSSART, P. & GIRARDIN, S. E. 2007. A critical role for
625 peptidoglycan N-deacetylation in *Listeria* evasion from the host innate immune
626 system. *Proc Natl Acad Sci U S A,* 104**,** 997-1002.
627 BOYLE, D. S., KHATTAR, M. M., ADDINALL, S. G., LUTKENHAUS, J. & DONACHIE, W. D. 1997.
628 *ftsW* is an essential cell-division gene in *Escherichia coli*. *Mol Microbiol,* 24**,** 1263-73.
629 BURKE, T. P., LOUKITCHEVA, A., ZEMANSKY, J., WHEELER, R., BONECA, I. G. & PORTNOY, D.
630 A. 2014. *Listeria monocytogenes* is resistant to lysozyme through the regulation, not
631 the acquisition, of cell wall-modifying enzymes. *J Bacteriol,* 196**,** 3756-67.
632 CARBALLIDO-LOPEZ, R. & FORMSTONE, A. 2007. Shape determination in *Bacillus subtilis*.
633 *Curr Opin Microbiol,* 10**,** 611-6.
634 CHO, H., WIVAGG, C. N., KAPOOR, M., BARRY, Z., ROHS, P. D. A., SUH, H., MARTO, J. A.,
635 GARNER, E. C. & BERNHARDT, T. G. 2016. Bacterial cell wall biogenesis is mediated
636 by SEDS and PBP polymerase families functioning semi-autonomously. *Nature*
637 *Microbiology,* 1**,** 16172.
638 CORRIGAN, R. M., ABBOTT, J. C., BURHENNE, H., KAEVER, V. & GRÜNDLING, A. 2011. c-di-
639 AMP is a new second messenger in *Staphylococcus aureus* with a role in controlling
640 cell size and envelope stress. *PLoS Pathog,* 7**,** e1002217.
641 DANIEL, R. A., WILLIAMS, A. M. & ERRINGTON, J. 1996. A complex four-gene operon
642 containing essential cell division gene *pbpB* in *Bacillus subtilis*. *J Bacteriol,* 178**,** 2343-
643 50.
644 DE JONGE, B. L., CHANG, Y. S., GAGE, D. & TOMASZ, A. 1992. Peptidoglycan composition of a
645 highly methicillin-resistant *Staphylococcus aureus* strain. The role of penicillin
646 binding protein 2A. *J Biol Chem,* 267**,** 11248-54.
647 DE PEDRO, M. A. & CAVA, F. 2015. Structural constraints and dynamics of bacterial cell wall
648 architecture. *Front Microbiol,* 6**,** 449.
649 DEN BLAAUWEN, T. 2018. Is Longitudinal Division in Rod-Shaped Bacteria a Matter of
650 Swapping Axis? *Front Microbiol,* 9**,** 822.
651 EMAMI, K., GUYET, A., KAWAI, Y., DEVI, J., WU, L. J., ALLENBY, N., DANIEL, R. A. &
652 ERRINGTON, J. 2017. RodA as the missing glycosyltransferase in *Bacillus subtilis* and
653 antibiotic discovery for the peptidoglycan polymerase pathway. *Nat Microbiol,* 2**,**
654 16253.
655 ERRINGTON, J. & WU, L. J. 2017. Cell Cycle Machinery in Bacillus subtilis. *In:* LÖWE, J. &
656 AMOS, L. A. (eds.) *Prokaryotic Cytoskeletons: Filamentous Protein Polymers Active in*
657 *the Cytoplasm of Bacterial and Archaeal Cells.* Cham: Springer International
658 Publishing.

659 FRAIPONT, C., ALEXEEVA, S., WOLF, B., VAN DER PLOEG, R., SCHLOESSER, M., DEN
660 BLAAUWEN, T. & NGUYEN-DISTECHE, M. 2011. The integral membrane FtsW protein
661 and peptidoglycan synthase PBP3 form a subcomplex in *Escherichia coli*.
662 *Microbiology,* 157**,** 251-9.
663 GAMBA, P., HAMOEN, L. W. & DANIEL, R. A. 2016. Cooperative Recruitment of FtsW to the
664 Division Site of *Bacillus subtilis*. *Front Microbiol,* 7**,** 1808.
665 GAMBA, P., VEENING, J. W., SAUNDERS, N. J., HAMOEN, L. W. & DANIEL, R. A. 2009. Two-
666 step assembly dynamics of the *Bacillus subtilis* divisome. *J Bacteriol,* 191**,** 4186-94.
667 GHUYSEN, J. M. & STROMINGER, J. L. 1963. Structure of the Cell Wall of *Staphylococcus*
668 *aureus*, Strain Copenhagen. Ii. Separation and Structure of Disaccharides.
669 *Biochemistry,* 2**,** 1119-25.
670 GOFFIN, C. & GHUYSEN, J. M. 1998. Multimodular penicillin-binding proteins: an enigmatic
671 family of orthologs and paralogs. *Microbiol Mol Biol Rev,* 62**,** 1079-93.
672 GOTTSCHALK, S., BYGEBJERG-HOVE, I., BONDE, M., NIELSEN, P. K., NGUYEN, T. H.,
673 GRAVESEN, A. & KALLIPOLITIS, B. H. 2008. The two-component system CesRK
674 controls the transcriptional induction of cell envelope-related genes in *Listeria*
675 *monocytogenes* in response to cell wall-acting antibiotics. *J Bacteriol,* 190**,** 4772-6.
676 GRÜNDLING, A., BURRACK, L. S., BOUWER, H. G. & HIGGINS, D. E. 2004. *Listeria*
677 *monocytogenes* regulates flagellar motility gene expression through MogR, a
678 transcriptional repressor required for virulence. *Proc Natl Acad Sci U S A,* 101**,** 12318-
679 23.
680 HARA, H. & SUZUKI, H. 1984. A novel glycan polymerase that synthesizes uncross-linked
681 peptidoglycan in *Escherichia coli*. *FEBS Lett,* 168**,** 155-60.
682 HENRIQUES, A. O., DE LENCASTRE, H. & PIGGOT, P. J. 1992. A *Bacillus subtilis* morphogene
683 cluster that includes *spoVE* is homologous to the *mra* region of *Escherichia coli*.
684 *Biochimie,* 74**,** 735-48.
685 HENRIQUES, A. O., GLASER, P., PIGGOT, P. J. & MORAN, C. P., JR. 1998. Control of cell shape
686 and elongation by the *rodA* gene in *Bacillus subtilis*. *Mol Microbiol,* 28**,** 235-47.
687 HÖLTJE, J. V. 1998. Growth of the stress-bearing and shape-maintaining murein sacculus of
688 *Escherichia coli*. *Microbiol Mol Biol Rev,* 62**,** 181-203.
689 IKEDA, M., SATO, T., WACHI, M., JUNG, H. K., ISHINO, F., KOBAYASHI, Y. & MATSUHASHI, M.
690 1989. Structural similarity among *Escherichia coli* FtsW and RodA proteins and
691 *Bacillus subtilis* SpoVE protein, which function in cell division, cell elongation, and
692 spore formation, respectively. *J Bacteriol,* 171**,** 6375-8.
693 JONES, L. J., CARBALLIDO-LOPEZ, R. & ERRINGTON, J. 2001. Control of cell shape in bacteria:
694 helical, actin-like filaments in *Bacillus subtilis*. *Cell,* 104**,** 913-22.
695 KALLIPOLITIS, B. H., INGMER, H., GAHAN, C. G., HILL, C. & SOGAARD-ANDERSEN, L. 2003.
696 CesRK, a two-component signal transduction system in *Listeria monocytogenes*,
697 responds to the presence of cell wall-acting antibiotics and affects beta-lactam
698 resistance. *Antimicrob Agents Chemother,* 47**,** 3421-9.
699 KARIMOVA, G., PIDOUX, J., ULLMANN, A. & LADANT, D. 1998. A bacterial two-hybrid system
700 based on a reconstituted signal transduction pathway. *Proc Natl Acad Sci U S A,* 95**,**
701 5752-6.
702 KARINOU, E., SCHUSTER, C. F., PAZOS, M., VOLLMER, W. & GRÜNDLING, A. 2018.
703 Inactivation of the monofunctional peptidoglycan glycosyltransferase SgtB allows
704 *Staphylococcus aureus* to survive in the absence of lipoteichoic acid. *J Bacteriol*.

705 KHATTAR, M. M., BEGG, K. J. & DONACHIE, W. D. 1994. Identification of FtsW and
706 characterization of a new *ftsW* division mutant of *Escherichia coli*. *J Bacteriol,* 176**,**
707 7140-7.
708 KOBAYASHI, K., EHRLICH, S. D., ALBERTINI, A., AMATI, G., ANDERSEN, K. K., ARNAUD, M.,
709 ASAI, K., ASHIKAGA, S., AYMERICH, S., BESSIERES, P., BOLAND, F., BRIGNELL, S. C.,
710 BRON, S., BUNAI, K., CHAPUIS, J., CHRISTIANSEN, L. C., DANCHIN, A., DEBARBOUILLE,
711 M., DERVYN, E., DEUERLING, E., DEVINE, K., DEVINE, S. K., DREESEN, O., ERRINGTON,
712 J., FILLINGER, S., FOSTER, S. J., FUJITA, Y., GALIZZI, A., GARDAN, R., ESCHEVINS, C.,
713 FUKUSHIMA, T., HAGA, K., HARWOOD, C. R., HECKER, M., HOSOYA, D., HULLO, M. F.,
714 KAKESHITA, H., KARAMATA, D., KASAHARA, Y., KAWAMURA, F., KOGA, K., KOSKI, P.,
715 KUWANA, R., IMAMURA, D., ISHIMARU, M., ISHIKAWA, S., ISHIO, I., LE COQ, D.,
716 MASSON, A., MAUEL, C., MEIMA, R., MELLADO, R. P., MOIR, A., MORIYA, S.,
717 NAGAKAWA, E., NANAMIYA, H., NAKAI, S., NYGAARD, P., OGURA, M., OHANAN, T.,
718 O'REILLY, M., O'ROURKE, M., PRAGAI, Z., POOLEY, H. M., RAPOPORT, G., RAWLINS, J.
719 P., RIVAS, L. A., RIVOLTA, C., SADAIE, A., SADAIE, Y., SARVAS, M., SATO, T., SAXILD, H.
720 H., SCANLAN, E., SCHUMANN, W., SEEGERS, J. F., SEKIGUCHI, J., SEKOWSKA, A.,
721 SEROR, S. J., SIMON, M., STRAGIER, P., STUDER, R., TAKAMATSU, H., TANAKA, T.,
722 TAKEUCHI, M., THOMAIDES, H. B., VAGNER, V., VAN DIJL, J. M., WATABE, K., WIPAT,
723 A., YAMAMOTO, H., YAMAMOTO, M., YAMAMOTO, Y., YAMANE, K., YATA, K.,
724 YOSHIDA, K., YOSHIKAWA, H., ZUBER, U. & OGASAWARA, N. 2003. Essential *Bacillus*
725 *subtilis* genes. *Proc Natl Acad Sci U S A,* 100**,** 4678-83.
726 KORSAK, D., MARKIEWICZ, Z., GUTKIND, G. O. & AYALA, J. A. 2010. Identification of the full
727 set of *Listeria monocytogenes* penicillin-binding proteins and characterization of
728 PBPD2 (Lmo2812). *BMC Microbiol,* 10**,** 239.
729 LECLERCQ, S., DEROUAUX, A., OLATUNJI, S., FRAIPONT, C., EGAN, A. J., VOLLMER, W.,
730 BREUKINK, E. & TERRAK, M. 2017. Interplay between Penicillin-binding proteins and
731 SEDS proteins promotes bacterial cell wall synthesis. *Sci Rep,* 7**,** 43306.
732 LIU, X., GALLAY, C., KJOS, M., DOMENECH, A., SLAGER, J., VAN KESSEL, S. P., KNOOPS, K.,
733 SORG, R. A., ZHANG, J. R. & VEENING, J. W. 2017. High-throughput CRISPRi
734 phenotyping identifies new essential genes in *Streptococcus pneumoniae*. *Mol Syst*
735 *Biol,* 13**,** 931.
736 LOBEL, L. & HERSKOVITS, A. A. 2016. Systems Level Analyses Reveal Multiple Regulatory
737 Activities of CodY Controlling Metabolism, Motility and Virulence in *Listeria*
738 *monocytogenes*. *PLoS Genet,* 12**,** e1005870.
739 MCPHERSON, D. C. & POPHAM, D. L. 2003. Peptidoglycan synthesis in the absence of class A
740 penicillin-binding proteins in *Bacillus subtilis*. *J Bacteriol,* 185**,** 1423-31.
741 MEESKE, A. J., RILEY, E. P., ROBINS, W. P., UEHARA, T., MEKALANOS, J. J., KAHNE, D.,
742 WALKER, S., KRUSE, A. C., BERNHARDT, T. G. & RUDNER, D. Z. 2016. SEDS proteins
743 are a widespread family of bacterial cell wall polymerases. *Nature,* 537**,** 634-638.
744 MEESKE, A. J., SHAM, L. T., KIMSEY, H., KOO, B. M., GROSS, C. A., BERNHARDT, T. G. &
745 RUDNER, D. Z. 2015. MurJ and a novel lipid II flippase are required for cell wall
746 biogenesis in *Bacillus subtilis*. *Proc Natl Acad Sci U S A,* 112**,** 6437-42.
747 NAKAGAWA, J., TAMAKI, S. & MATSUHASHI, M. 1979. Purified penicillin binding proteins 1Bs
748 from *Escherichia coli* membrane showing activities of both peptidoglycan
749 polymerase and peptidoglycan crosslinking enzyme. *Agric. Biol. Chem.,* 43**,** 1379-
750 1380.

751 NANNINGA, N. 1991. Cell division and peptidoglycan assembly in *Escherichia coli*. *Mol*
752 *Microbiol,* 5**,** 791-5.
753 NIELSEN, P. K., ANDERSEN, A. Z., MOLS, M., VAN DER VEEN, S., ABEE, T. & KALLIPOLITIS, B. H.
754 2012. Genome-wide transcriptional profiling of the cell envelope stress response and
755 the role of LisRK and CesRK in *Listeria monocytogenes*. *Microbiology,* 158**,** 963-74.
756 PARK, W. & MATSUHASHI, M. 1984. *Staphylococcus aureus* and *Micrococcus luteus*
757 peptidoglycan transglycosylases that are not penicillin-binding proteins. *J Bacteriol,*
758 157**,** 538-44.
759 PARK, W., SETO, H., HAKENBECK, R. & MATSUHASHI, M. 1985. Major peptidoglycan
760 transglycosylase activity in *Streptococcus pneumoniae* that is not a penicillin-binding
761 protein. *FEMS Microbiology Letters,* 27**,** 45-48.
762 PINHO, M. G., KJOS, M. & VEENING, J. W. 2013. How to get (a)round: mechanisms
763 controlling growth and division of coccoid bacteria. *Nat Rev Microbiol,* 11**,** 601-14.
764 REICHMANN, N. T., TAVARES, A. C., SARAIVA, B. M., JOUSSELIN, A., REED, P., PEREIRA, A. R.,
765 MONTEIRO, J. M., SOBRAL, R. G., VANNIEUWENHZE, M. S., FERNANDES, F. & PINHO,
766 M. G. 2019. SEDS-bPBP pairs direct lateral and septal peptidoglycan synthesis in
767 *Staphylococcus aureus*. *Nat Microbiol*.
768 RISMONDO, J., MÖLLER, L., ALDRIDGE, C., GRAY, J., VOLLMER, W. & HALBEDEL, S. 2015.
769 Discrete and overlapping functions of peptidoglycan synthases in growth, cell
770 division and virulence of *Listeria monocytogenes*. *Mol Microbiol,* 95**,** 332-51.
771 ROGERS, H. J., PERKINS, H. R. & WARD, J. B. 1980. Microbial Cell Walls and Membranes.
772 *Chapman and Hall New York, N.Y.,* 10**,** 33-33.
773 RUIZ, N. 2008. Bioinformatics identification of MurJ (MviN) as the peptidoglycan lipid II
774 flippase in *Escherichia coli*. *Proc Natl Acad Sci U S A,* 105**,** 15553-7.
775 SAUVAGE, E., KERFF, F., TERRAK, M., AYALA, J. A. & CHARLIER, P. 2008. The penicillin-binding
776 proteins: structure and role in peptidoglycan biosynthesis. *FEMS Microbiol Rev,* 32**,**
777 234-58.
778 SCHEFFERS, D. J. & PINHO, M. G. 2005. Bacterial cell wall synthesis: new insights from
779 localization studies. *Microbiol Mol Biol Rev,* 69**,** 585-607.
780 SHAM, L. T., BUTLER, E. K., LEBAR, M. D., KAHNE, D., BERNHARDT, T. G. & RUIZ, N. 2014.
781 Bacterial cell wall. MurJ is the flippase of lipid-linked precursors for peptidoglycan
782 biogenesis. *Science,* 345**,** 220-2.
783 SIEVERS, F., WILM, A., DINEEN, D., GIBSON, T. J., KARPLUS, K., LI, W., LOPEZ, R., MCWILLIAM,
784 H., REMMERT, M., SODING, J., THOMPSON, J. D. & HIGGINS, D. G. 2011. Fast,
785 scalable generation of high-quality protein multiple sequence alignments using
786 Clustal Omega. *Mol Syst Biol,* 7**,** 539.
787 SONNHAMMER, E. L., VON HEIJNE, G. & KROGH, A. 1998. A hidden Markov model for
788 predicting transmembrane helices in protein sequences. *Proc Int Conf Intell Syst Mol*
789 *Biol,* 6**,** 175-82.
790 STONE, K. J. & STROMINGER, J. L. 1971. Mechanism of action of bacitracin: complexation
791 with metal ion and C 55 -isoprenyl pyrophosphate. *Proc Natl Acad Sci U S A,* 68**,**
792 3223-7.
793 SWAMINATHAN, B. & GERNER-SMIDT, P. 2007. The epidemiology of human listeriosis.
794 *Microbes Infect,* 9**,** 1236-43.
795 TAGUCHI, A., WELSH, M. A., MARMONT, L. S., LEE, W., SJODT, M., KRUSE, A. C., KAHNE, D.,
796 BERNHARDT, T. G. & WALKER, S. 2019. FtsW is a peptidoglycan polymerase that is

797 functional only in complex with its cognate penicillin-binding protein. *Nat Microbiol,*
798 4**,** 587-594.
799 TAMURA, T., SUZUKI, H., NISHIMURA, Y., MIZOGUCHI, J. & HIROTA, Y. 1980. On the process
800 of cellular division in *Escherichia coli*: isolation and characterization of penicillin-
801 binding proteins 1a, 1b, and 3. *Proc Natl Acad Sci U S A,* 77**,** 4499-503.
802 TOLEDO-ARANA, A., DUSSURGET, O., NIKITAS, G., SESTO, N., GUET-REVILLET, H.,
803 BALESTRINO, D., LOH, E., GRIPENLAND, J., TIENSUU, T., VAITKEVICIUS, K.,
804 BARTHELEMY, M., VERGASSOLA, M., NAHORI, M. A., SOUBIGOU, G., REGNAULT, B.,
805 COPPEE, J. Y., LECUIT, M., JOHANSSON, J. & COSSART, P. 2009. The *Listeria*
806 transcriptional landscape from saprophytism to virulence. *Nature,* 459**,** 950-6.
807 TYPAS, A., BANZHAF, M., GROSS, C. A. & VOLLMER, W. 2012. From the regulation of
808 peptidoglycan synthesis to bacterial growth and morphology. *Nat Rev Microbiol,* 10**,**
809 123-36.
810 VAN HEIJENOORT, J. 2001. Formation of the glycan chains in the synthesis of bacterial
811 peptidoglycan. *Glycobiology,* 11**,** 25R-36R.
812 VAN HEIJENOORT, Y., LEDUC, M., SINGER, H. & VAN HEIJENOORT, J. 1987. Effects of
813 moenomycin on *Escherichia coli*. *J Gen Microbiol,* 133**,** 667-74.
814 VOLLMER, W., BLANOT, D. & DE PEDRO, M. A. 2008. Peptidoglycan structure and
815 architecture. *FEMS Microbiol Rev,* 32**,** 149-67.
816 WANG, Q. M., PEERY, R. B., JOHNSON, R. B., ALBORN, W. E., YEH, W. K. & SKATRUD, P. L.
817 2001. Identification and characterization of a monofunctional glycosyltransferase
818 from *Staphylococcus aureus*. *J Bacteriol,* 183**,** 4779-85.
819 WEI, Y., HAVASY, T., MCPHERSON, D. C. & POPHAM, D. L. 2003. Rod shape determination by
820 the *Bacillus subtilis* class B penicillin-binding proteins encoded by *pbpA* and *pbpH*. *J*
821 *Bacteriol,* 185**,** 4717-26.
822 WEIDEL, W. & PELZER, H. 1964. Bagshaped Macromolecules--a New Outlook on Bacterial
823 Cell Walls. *Adv Enzymol Relat Areas Mol Biol,* 26**,** 193-232.
824 ZHANG, C., NIETFELDT, J., ZHANG, M. & BENSON, A. K. 2005. Functional consequences of
825 genome evolution in *Listeria monocytogenes*: the *lmo0423* and *lmo0422* genes
826 encode sigmaC and LstR, a lineage II-specific heat shock system. *J Bacteriol,* 187**,**
827 7243-53.
828

Table 1: Sequence homology between *B. subtilis* and *L. monocytogenes* FtsW/RodA proteins as determined by BLAST.

***L. monocytogenes* proteins**	***B. subtilis* FtsW (403 aa)***	***B. subtilis* RodA (393 aa)***
Lmo0421	46/128 aa (36%)	77/350 aa (22%)
(416 aa)	7e-14	4e-09
FtsW1 (Lmo1071)	195/403 aa (48%)	100/333 aa (30%)
(402 aa)	1e-122	7e-35
RodA1 (Lmo2427)	124/403 aa (31%)	132/360 aa (37%)
(391 aa)	9e-29	1e-57
RodA2 (Lmo2428)	112/374 aa (30%)	159/402 aa (40%)
(389 aa)	1e-33	1e-66
RodA3 (Lmo2687)	95/324 aa (29%)	110/356 aa (31%)
(369 aa)	3e-25	3e-44
FtsW2 (Lmo2688)	147/342 aa (43%)	95/300 aa (32%)
(376 aa)	5e-67	6e-22

* *L. monocytogenes* proteins and their amino acid sizes (aa) are shown in bold in the left column and *B. subtilis* FtsW and RodA proteins used for the homology search are denoted in the top row. The number of amino acids, which were found to be identical between the respective *L. monocytogenes* and *B. subtilis* FtsW/RodA protein are denoted (left number) along with the amino acids that was utilized by the BLAST algorithm for this comparison (right number). The % identity is given in brackets and the corresponding e-values are indicated below.

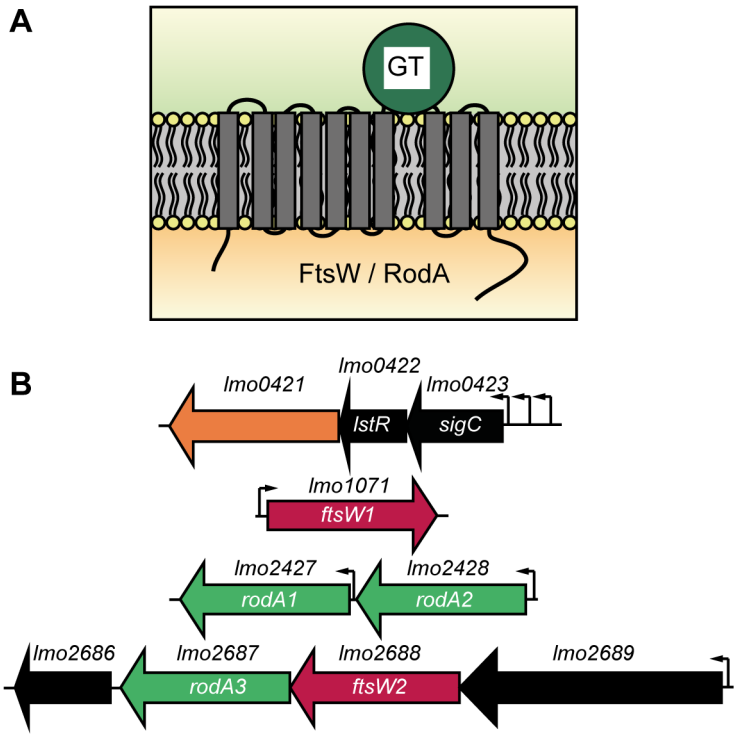

Figure 1: Topology of FtsW and RodA enzymes and their genomic arrangement in *L. monocytogenes*. (A) Topology models for FtsW and RodA enzymes of *L. monocytogenes* as predicted using the TMHMM v. 2.0 server (Sonnhammer et al., 1998). (B) Genomic organization of *ftsW/rodA* genes in *L. monocytogenes.* Arrowheads indicate the gene orientation. Small black arrows indicate promoters based on the operon structures described in Toledo-Arana *et al*. (Toledo-Arana et al., 2009). Three different promoters have been identified for the *sigC* operon (Zhang et al., 2005).

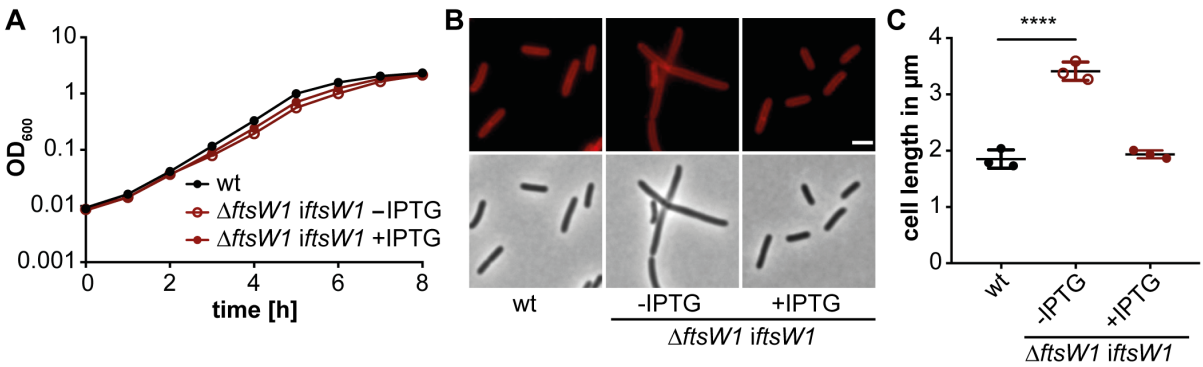

Inserted Δ*ftsW1 in figure to have it match with the legend*

Figure 2: Depletion of FtsW1 results in cell elongation. (A) Growth of the *L. monocytogenes* FtsW1 depletion strain. Strain 10403SΔ*ftsW1* i*ftsW1* was grown overnight in BHI medium in the presence of 1 mM IPTG. The following day, the cells were washed and used to inoculate fresh BHI medium without IPTG and incubated at 37°C for 8-10h, diluted again and grown until the next morning. The depletion culture was used to inoculate BHI medium without IPTG or with 1 mM IPTG and the growth was monitored by determining OD_{600} readings at hourly intervals. Wild type *L. monocytogenes* strain 10403S (wt) was used as control. Averages and standard deviations from three independent experiments were plotted. Of note, due to the small standard deviations the actual error bars are not visible in the graph. (B) Microscopy analysis of 10403S (wt) and the *ftsW1* depletion strain grown in the presence or absence of IPTG. For depletion of FtsW1, strain 10403SΔ*ftsW1* i*ftsW1* was grown as described in panel A. Cultures of 10403S and 10403SΔ*ftsW1* i*ftsW1* were diluted 1:100 in fresh BHI medium (with 1 mM IPTG where indicated), grown for 3 h at 37°C and the cells subsequently stained with the membrane dye nile red and analyzed by fluorescence and phase contrast microscopy. The scale bar is 2 µm. (C) Cell lengths measurement of 10403S (wt) and the *ftsW1* depletion strain. The cell length of 300 cells per strain was measured and the median cell length calculated and plotted. Three independent experiments were performed, and the average and standard deviation of the median cell length plotted. For

statistical analysis, a one-way ANOVA coupled with a Dunnett's multiple comparisons test was performed (**** $p \leq 0.0001$).

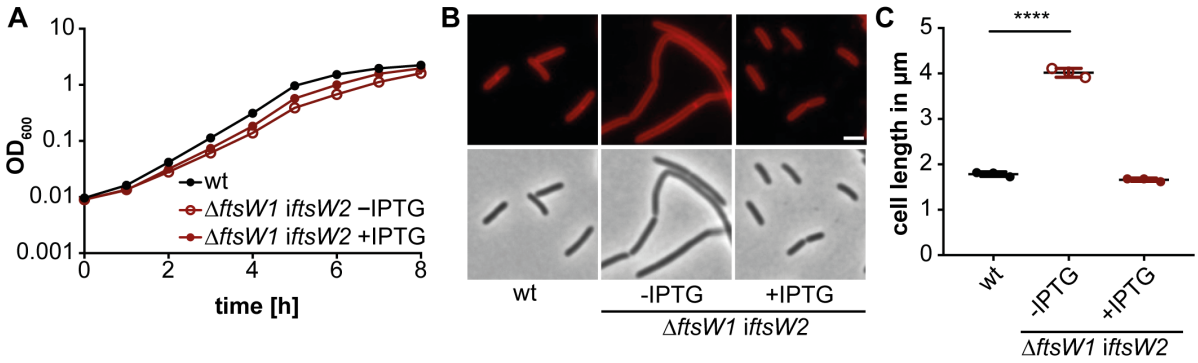

Fig. 3: Overexpression of FtsW2 can compensate for the loss of FtsW1. (A) Growth comparison of strains 10403S (wt) and 10403SΔ*ftsW1* i*ftsW2*. Growth curves were performed as described in Figure 2. (B) Microscopy images of strains 10403S (wt) and 10403SΔ*ftsW1* i*ftsW2*. For depletion of FtsW2, strain 10403SΔ*ftsW1* i*ftsW2* was grown as described in Figure 2. The next morning, cells were diluted 1:100 and grown in BHI broth (with or without IPTG as indicated) until mid-logarithmic growth phase, stained with the membrane dye nile red and subjected to fluorescence and phase contrast microscopy analysis. Scale bar is 2 µm. (C) Cell lengths measurements of 10403S (wt) and 10403SΔ*ftsW1* i*ftsW2*. The cell length of 300 cells per strain was measured and the median cell length calculated and plotted. Three independent experiments were performed, and the average and standard deviation of the median cell length plotted. For statistical analysis, a one-way ANOVA coupled with a Dunnett's multiple comparisons test was performed (**** $p \leq 0.0001$).

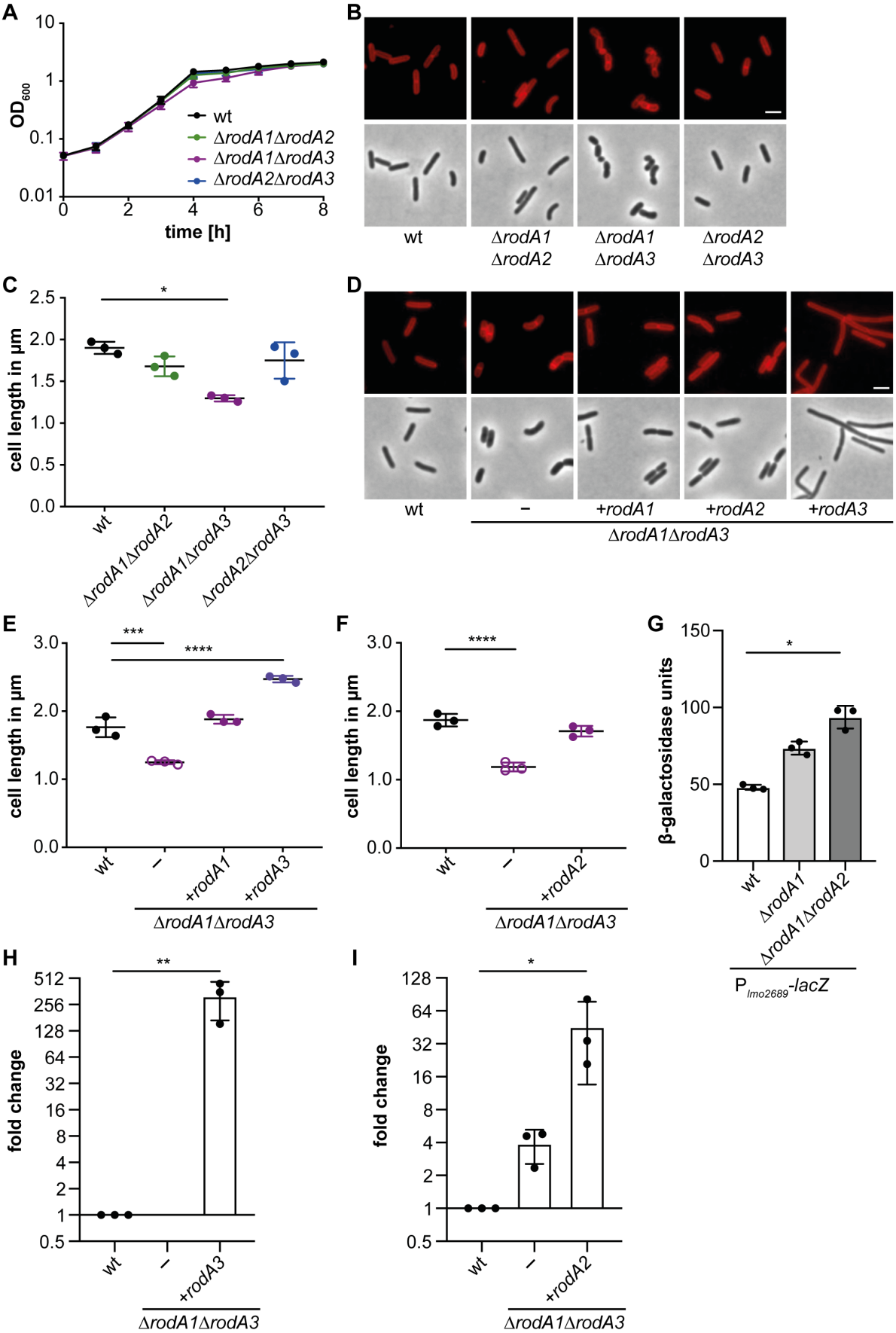
A
OD600
time [h]
wt
ΔrodA1ΔrodA2
ΔrodA1ΔrodA3
ΔrodA2ΔrodA3
B
wt
ΔrodA1 ΔrodA2
ΔrodA1 ΔrodA3
ΔrodA2 ΔrodA3
C
cell length in µm
D
wt
–
+rodA1
+rodA2
+rodA3
ΔrodA1ΔrodA3
E
cell length in µm
F
cell length in µm
G
β-galactosidase units
P lmo2689-lacZ
H
fold change
I
fold change

Fig. 4: RodA1 and RodA3 are essential to maintain the rod shape of *L. monocytogenes*. (A) Growth of *L. monocytogenes* 10403S (wt), 10403SΔ*rodA1*Δ*rodA2*, 10403SΔ*rodA1*Δ*rodA3* and 10403SΔ*rodA2*Δ*rodA3* strains in BHI broth at 37°C. (B) Microscopy images of wt and mutant *L. monocytogenes* strains. Cells from the strains described in panel A were stained with the membrane dye nile red and analyzed by fluorescence and phase contrast microscopy. Scale bar is 2 µm. (C) Cell lengths measurements of wt and mutant *L. monocytogenes* strains. The cell length of 300 cells per strain was measured and the median cell length calculated and plotted. Three independent experiments were performed, and the average and standard deviation of the median cell length plotted. For statistical analysis, one-way ANOVA t-tests for multiple comparisons were used (** $p \leq 0.01$). (D) Microscopy images of wildtype and mutant *L. monocytogenes* strains. Cells from 10403S (wt), 10403SΔ*rodA1*Δ*rodA3* (-) and 10403SΔ*rodA1*Δ*rodA3* expressing *rodA1*, *rodA2* or *rodA3* from an IPTG-inducible promoter were stained with the membrane dye nile red and analyzed by fluorescence and phase contrast microscopy. Scale bar is 2 µm. (E-F) Cell length analysis of 10403SΔ*rodA1*Δ*rodA3* complementation strains. Analysis was performed as described in panel C. (G) β-galactosidase assay using *L. monocytogenes* strains 10403S (wt), 10403SΔ*rodA1* and 10403SΔ*rodA1-2* carrying a $P_{lmo2689}$-*lacZ* fusion construct. Averages and standard deviations of three independent experiments were plotted. For statistical analysis, a one-way ANOVA coupled with a Dunnett's multiple comparisons test was used (* $p \leq 0.1$). (H) Analysis of *rodA3* expression by qRT-PCR. RNA was isolated from strains 10403S (wt), 10403SΔ*rodA1*Δ*rodA3* (-) and 10403SΔ*rodA1*Δ*rodA3* i*rodA3* grown in the presence of IPTG. Expression of *rodA3* was normalized to the expression of *gyrB* and fold changes calculated using the ΔΔCt method. Averages and standard deviations of three independent experiments were plotted. For statistical analysis, a one-way ANOVA coupled with a Dunnett's multiple comparisons test

was performed (** $p \leq 0.01$). (I) Analysis of *rodA2* expression using qRT-PCR. Same as panel (H) but using strains 10403S, 10403SΔ*rodA1*Δ*rodA3* (-) and 10403SΔ*rodA1*Δ*rodA3* i*rodA2* grown in the presence of IPTG. Averages and standard deviations of three independent experiments were plotted. For statistical analysis, a one-way ANOVA coupled with a Dunnett's multiple comparisons test was performed (* $p \leq 0.05$).

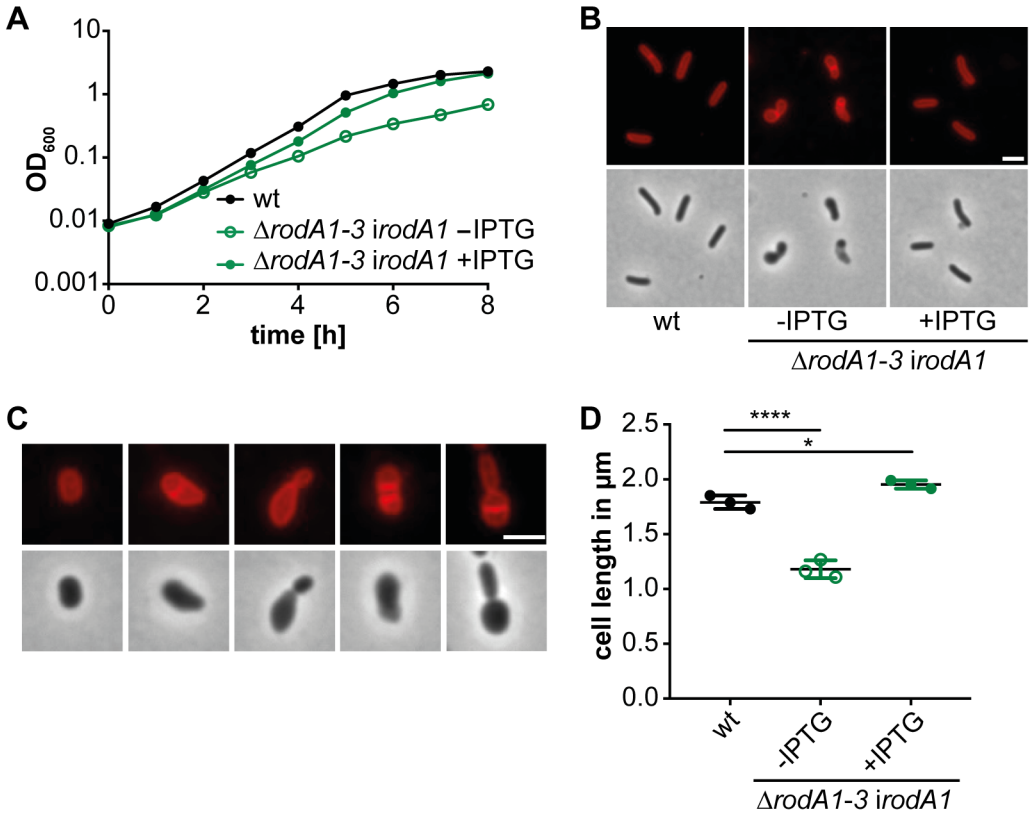

Figure 5: Absence of all three RodA proteins leads to a drastic cell shortening. (A) Growth of *L. monocytogenes* in the absence of all three RodA proteins. Growth curves were performed as described in Figure 2 using strain 10403S and strain 10403SΔ*rodA1-3* i*rodA1* grown in the presence of absence of IPTG. (B and C) Microscopy analysis of strain 10403SΔ*rodA1-3* i*rodA1*. For depletion of RodA1, strain 10403SΔ*rodA1-3* i*rodA1* was grown in the same way as described for the FtsW1 depletion in Figure 2. (B) Wildtype 10403S and depleted 10403SΔ*rodA1-3* i*rodA1* cultures were diluted 1:100, grown for 3 h at 37°C (where indicated in the presence of 1 mM IPTG), stained with nile red and phase contrast and fluorescence microscopy images were taken. Scale bar is 2 µm. (C) Microscopy images showing examples of different cell morphologies observed for strain 10403SΔ*rodA1-3* i*rodA1* depleted for RodA1. Scale bar is 2 µm. (D) Cell lengths measurements of 10403S (wt) and strain 10403SΔ*rodA1-3* i*rodA1*. The cell length of 300 cells per strain was measured. Three independent experiments were performed, and the average and standard deviation of the median cell length plotted. For statistical analysis, a one-way ANOVA

coupled with a Dunnett's multiple comparisons test was performed (* $p \leq 0.1$, **** $p \leq 0.0001$).

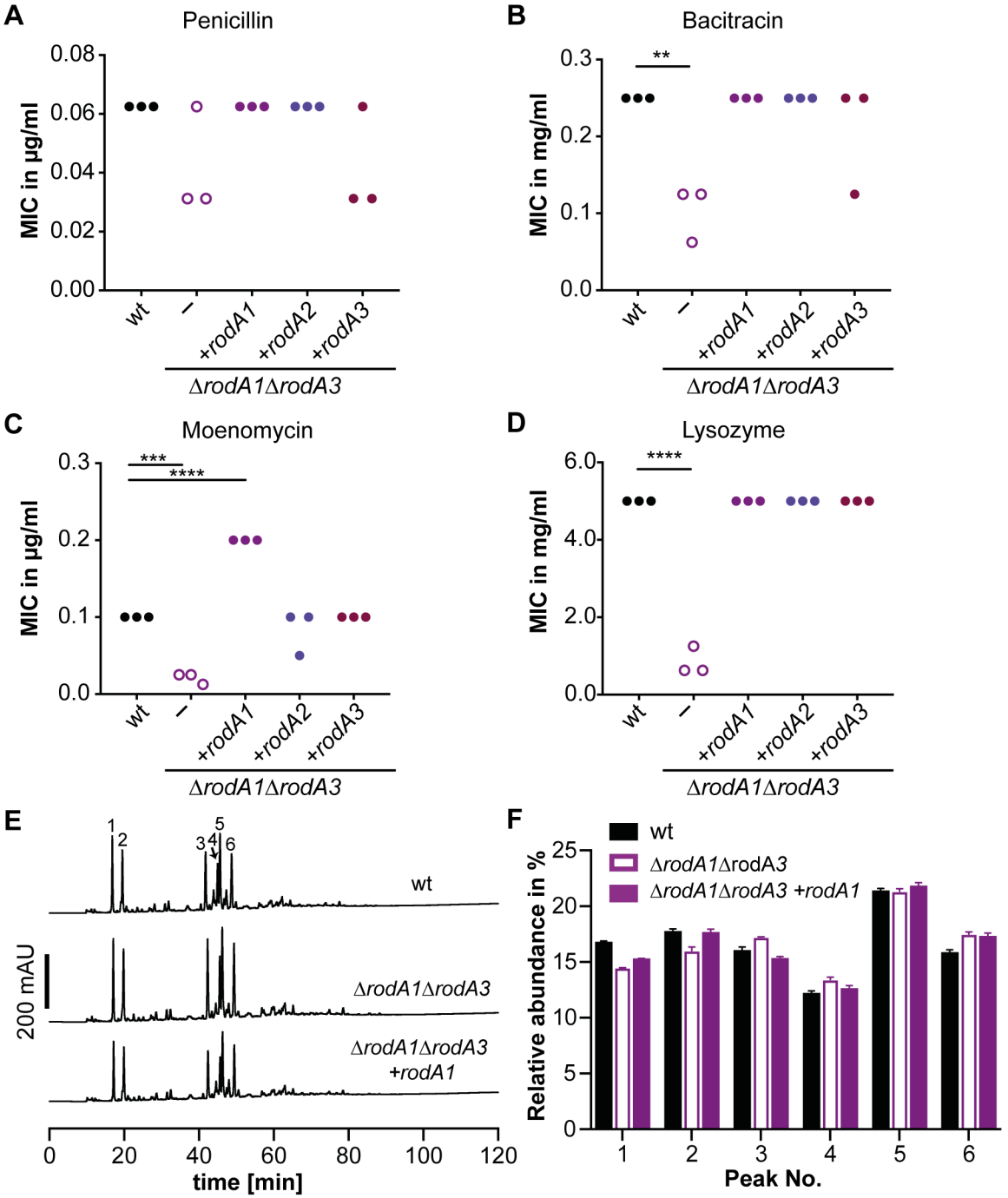

Figure 6: Impact of *rodA1* and *rodA3* deletion on the antibiotic and lysozyme resistance. The minimal inhibitory concentrations for the antibiotics penicillin G (A), bacitracin A (B), moenomycin (C) and lysozyme (D) were determined for the wildtype *L. monocytogenes* strain 10403S, the Δ*rodA1*Δ*rodA3* deletion strain and the complementation strains 10403SΔ*rodA1*Δ*rodA3* i*rodA1,* 10403SΔ*rodA1*Δ*rodA3* i*rodA2* and 10403SΔ*rodA1*Δ*rodA3* i*rodA3* using a microbroth dilution assay. The complementation strains were grown in the

presence of 1 mM IPTG. The result of three biological replicates are shown in A-D. For statistical analysis, a one-way ANOVA coupled with a Dunnett's multiple comparisons test was used (** $p \leq 0.01$, *** $p \leq 0.001$, **** $p \leq 0.0001$). (E) HPLC analysis of the muropeptide composition of 10403S (wt), 10403SΔ*rodA1*Δ*rodA3* and 10403SΔ*rodA1*Δ*rodA3* i*rodA1* (grown in the presence of IPTG to induce expression of RodA1). The major muropeptide peaks are numbered 1-6 as previously described (Rismondo et al., 2015, Burke et al., 2014). (F) Relative abundance of muropeptide peaks 1-6 in peptidoglycan isolated from strains 10403S (wt), 10403SΔ*rodA1*Δ*rodA3* and 10403SΔ*rodA1*Δ*rodA3* i*rodA1*. Average values and standard deviations were calculated from three independent peptidoglycan extractions.

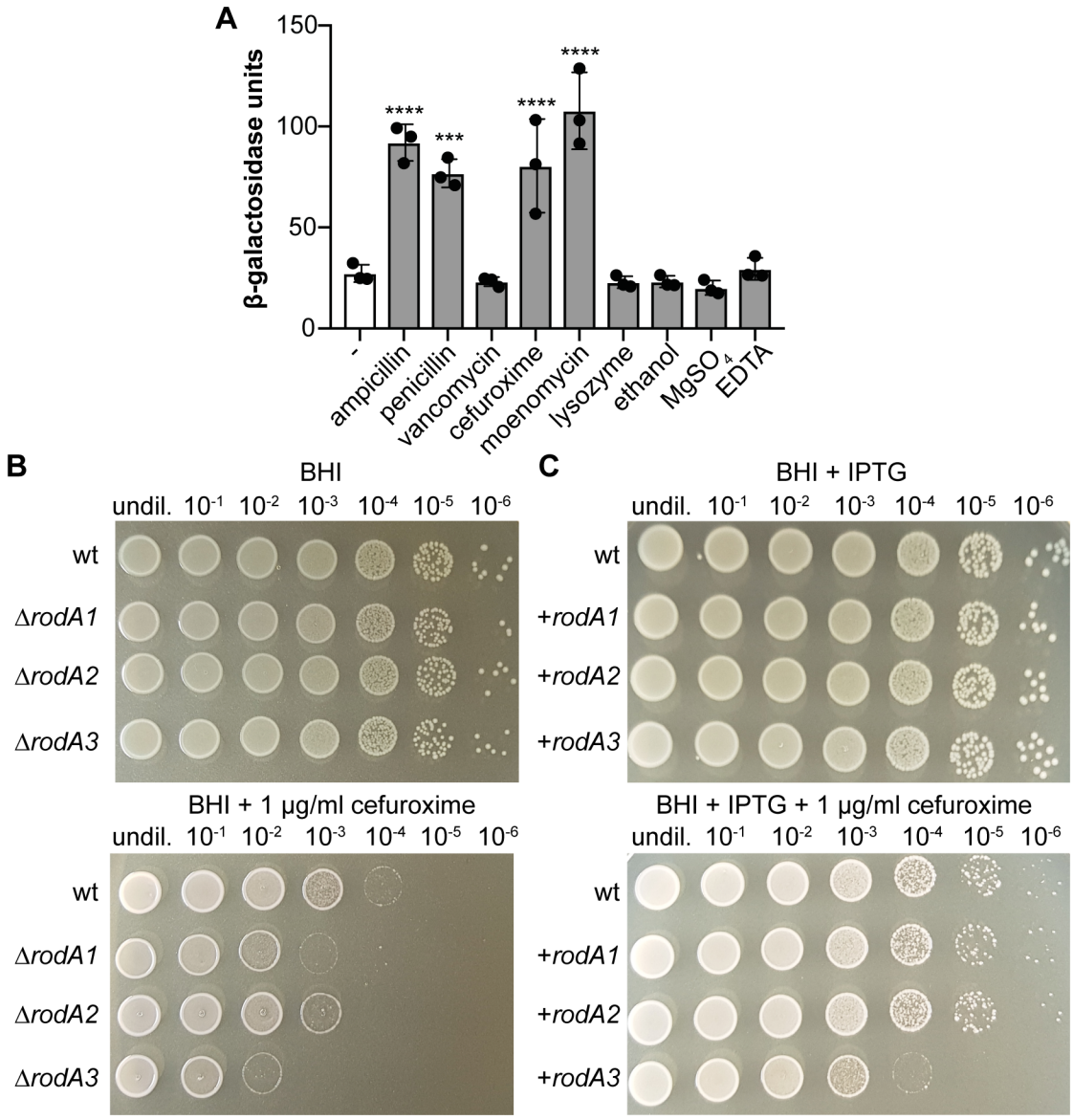

Figure 7: Cell wall-acting antibiotics increase the *lmo2689* promoter activity. (A) Bacteria from mid-logarithmic cultures of strain 10403S pPL3e-$P_{lmo2689}$-*lacZ* were exposed for 2 h at 37°C to different stressors. The activity of the *lmo2689* promoter was subsequently determined by performing β-galactosidase activity assays as described in the method section. Bacteria that had been grown in the absence of a stressor were included as negative (-) control. The averages of the β-galactosidase activity units and standard deviations from three independent experiments were plotted. For statistical analysis, a one-way ANOVA coupled with a Dunnett's multiple comparisons test was used (*** $p \leq 0.001$, **** $p \leq 0.0001$). (B) Absence and overexpression of RodA3 results in decreased cefuroxime resistance. Dilutions

of overnight cultures of strains (B) 10403S (wt), 10403SΔ*rodA1*, 10403SΔ*rodA2* and 10403SΔ*rodA3* and (C) 10403S (wt), 10403S pIMK3-*rodA1*, 10403S pIMK3-*rodA2* and 10403S pIMK3-*rodA3* were spotted on BHI agar and BHI agar containing 1 µg/ml cefuroxime and incubated for 24 h at 37°C. BHI agar plates were supplemented with 1 mM IPTG for cefuroxime resistance assays shown in panel C. A representative result from three independent experiments is shown.

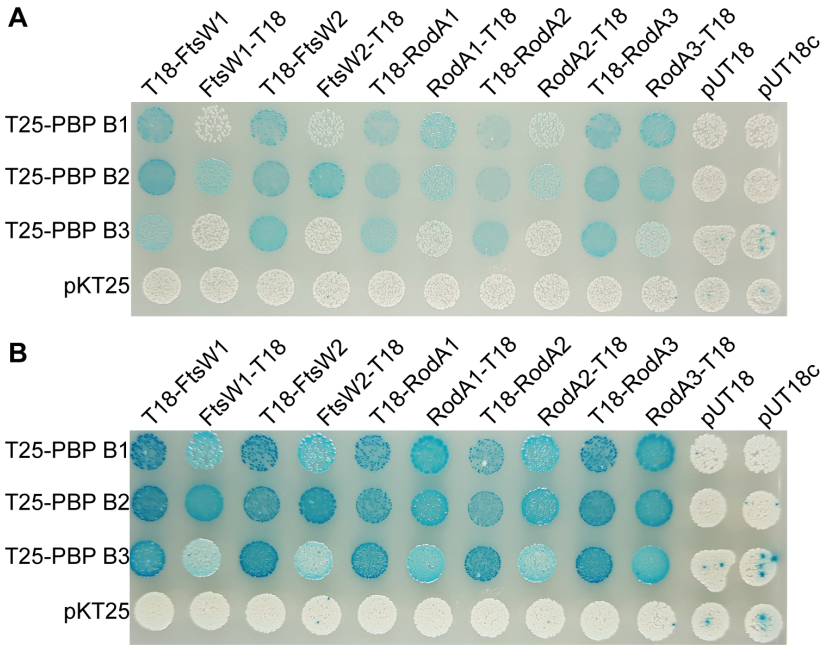

Figure 8: FtsW and RodA enzymes interact with class B PBPs. (A-B) FtsW/RodA and class B PBPs were fused to the T18 and T25-fragments of the *Bordetella pertussis* adenylate cyclase and co-transformed into the bacterial two-hybrid strain BTH101. Co-transformations with pKT25, pUT18 and pUT18c were used as negative controls. The plates were photographed after incubation at 30°C for (A) 24 h or (B) 48 h. Representative images from four independent experiments are shown.

```
Bsu RodA     ------------------------------------------------------------MSRYKKQQSPFYQGDLIFI 19
Bsu FtsW     ---------------------------------------------------------------MLKKMLKSYDY-SLIFA 16
Lmo0421      MSSSTFEEYLGKVIANVKSKQAHSMIKKELSNHLEELSHSFQKRGLSIEDANKKAMQEMGDPSTVGRNMNQLHKPRMDW-LLIAL 84
FtsW1        ------------------------------------------------------------MPMFKRILKSYDY-AFIAV 18
RodA1        ------------------------------------------------------------MNQQNKLAGRIDY-GIVLS 18
RodA2        ------------------------------------------------------------MARNRKKAVRIDY-SIIFL 18
RodA3        ---------------------------------------------------------------------MKRDVLYN-RIILS 13
FtsW2        ------------------------------------------------------------------------MRAGR-VLFVT 10
                                                                                                :.

Bsu RodA     FGVFFIISVVSIYAAGQF------GQYGNTDWIQQIVFYLLGAVAI-TVLLYFDLEQLEKLSLYIFIIGILSLIILKISPESIAP 97
Bsu FtsW     IVLLCGFGLVMVYSSSMITAVSRYGVSSNFFFMRQLFALIAGG-ALFILMALFPYKALAHQKFQKGI--LLVSVLALISLFVFGH 98
Lmo0421      FILLAGISFLPIIGD--------VVASNSSFMKKQIVWLAIAVLAL-IGFLFFDYRKLKDLWMYFYA----AALILFFTTFLVGI 156
FtsW1        FIVLCLFGLIMIYSASWSLAIG-KGLPADYFYARQVKNFIISF-IFFILFALLPFKFYQNNKVLMLI--VFGSIGVLLLIFLVGK 99
RodA1        MMLLMIISLVSIYSAQLTN-----NQYDANFVVKQAMWFVVSTFAI-IVVMQLDYDRLTKWAYYFYGL---GLFLL-VFVLLFGK 93
RodA2        MMLLCIIGLVAIYVAGLVN-----DQYTNNFLLQQSIWIVISTGVVVVIVLFFDYDKLQWAAYYLYGI---GNLLL-VLVLIVGD 94
RodA3        VFLLSLVSCVAIYFAQQT------NQYNTNFLGMQLVFLAIGTLTCF-GVSRLPIEFLRHHAIWLYVIMVITLLGI-LIPNPLVQ 90
FtsW2        YLLLAIWSLLLVYSTSYGVAVMRYKVEPSYFFNRQLLFYGLGF-LGLLVCSRINVQLFYLRRTLRIL--AGSLLGLLLLVLLTGS 92
               ::   . : :                        *      .          :                    .   .

Bsu RodA     VIKGAKSWFRIGRI-TIQPSEFMKVGLIMMLASVIGKANPKG-VRTLRDDIHLLLKIAGV---AVIPVGLILM-QDAGTAGICMF 174
Bsu FtsW     VAGNAQSWFKIGGM-SIQPGEFVKLVVILYLAAVYAKKQSYI-DHL-------LTGVAPPVVMTLIICGLIAMQPDFGTAMIIGL 174
Lmo0421      PLTGGGRWMSLWGI-AIDSPAISLFLFFIAWAGIFTKANAFKG----------WKKQVVLLIL--------FWVPVISYIIINRF 222
FtsW1        TVNNANSWLVLGPR-SLQPGEFAKLAVIIYMSAIYAKKQSYI-DDF-------NRGVLPPIFFLAFVCFLIAIQPDTGTAFIIFL 175
RodA1        EVKGAKSWIVIPFLGNIQPSEVVKVILIVVLAKVIWDHNRTYKIHRFSYDAWLLLKIGLF---TLMPLILIMLQPDLGTALVFIA 175
RodA2        ERKGSKSWISIGSLGSLQPSELMKSFLILALAKVIWDHNKKYKLHTVSLDMQLLLKIGIV---SILPLGLVALQPDLGTILVFIA 176
RodA3        NINGATRWYRFAGL-SFQPSEVVKSIFIFVLAHFAVK----Y-------QAQKWKQLGILTVLTGIVLLLIMKQPDLGTTIVYGV 163
FtsW2        AANNAQRWLSIAGV-TFQPTEMVKLLLILVIATVFLKKGCGV-RVQ-------Y----WLLGFLFLTVGLVFLQPDLGTALILGV 164
                .. *  :     ::   .    .:.  : .  .                                        .   :

Bsu RodA     IVLVMVFMSGINWKLIAIIAGSGILLISLILLVMINFPDV----------AKSVGIQDY-QIKRVTSWVSASNETQEDSNDSWQV 250
Bsu FtsW     IATCMILCSGFSGKTLVRLVILGGIVFILVSPIIYL--------------NQDKILTEG-RLARFESLEDPFKYANS---SGLQV 241
Lmo0421      VFSIM------------------YFLCVLVMYIFYYRHNRFAIKVALGNLLVGVIFISTMILKYPSSYLPDTSIPLK-------- 281
FtsW1        VGCCIIITSGMRLRTIMKLIGIGMGIIIGLTLILFALPDS----------VRNEIVSPT-KVARITTFMNPFEYADK---EGHQL 246
RodA1        IMSGMILISGITWKIIVPLFGSIAAIGTALIWMVIYHQNW----------LTSLGFKPY-QFERITTWINPENDPQ---GGGYQV 246
RodA2        IIIGMVFISGVTWKILLPVFSSIALIGGTLIYLVMYNQEF----------LQKLGFKPY-QFKRITSWLRPEEDPL---GDGMQL 247
RodA3        TALAIILLAIKSTKLMVGIITLILTAATIGMYVVVYHISL----------LEKIGFHAY-QFSRIQTWLDPTTDPD---A-VYQL 233
FtsW2        IGVALFLTSGVGLTRLVRVAIWTFGLLLLVAMLIYFF--------------HPDFFSSA-KLGRFA-FLDPFNLDNL--DASYQL 231
                :                            :.                    .     .

Bsu RodA     DQAIMAIGSGGILGNGISNL---KVYVPESTTDFIFSIIGESFGFIGCAIVVIMFFFLIYRLVVLIDKIHPFNRFASFFCVGYTA 332
Bsu FtsW     INSYYAISSGGIFGLGLGESIQKYGYLPESHTDFIMAVIAEELGIFGVLFVIFLLGFVVIKGFYIA--RKCEDPFGSLLAIGISS 324
Lmo0421      ----DILSKAGWFGKGLHN----NLILPEAHTDFVFPFLVYSLGWVFGIFLCLLLVVFILRISRNA--FKTKDLFGRLLTIGGAV 356
FtsW1        INSFYAIGSGGVSGQGLGESVQKLGYLPEAHTDFIIAVVAEELGVFGVMFIILALFFIIFKTITTG--LRAKDPFASLMCYGIAS 329
RodA1        LRAMTAIGSGQISGNGAGYD---AIAIPENHNDFIFTIVAGDYGFIGASILLAIYFLLIYQIIRVA--LDVGVPFYSYICTGVVM 326
RodA2        LRSMQAIGSGQLQGNGIGNQ---AIAIPENHNDFIFSIIGGNFGFIGGCVLIMLYFLLIYQIIRVA--LDINIPFYSYICTGVCS 327
RodA3        NLSMKAVGSGMMTGSSGT-----NAYIPESHTDMIFSTIGHQFGFVGVSLLLILFMVLIHQLIMAA--LLMKNTFSSLVLAGFAV 311
FtsW2        RNGYYAIGSGGIFGNGLGGSIQKLGYLPEPHTDFIMTVIAEELGVFGVIWTIFLLMALSFTALYIA--ISSHFIFDSMVCIGVAS 314
                   :...   * .          :**  .*:::  :  . * .           .                *   .  *

Bsu RodA     LIVIHTFQNIGMNIGIMPVTGIPLLFVSYGGSSTLSTLIGFGIVYNASVQLTKYRSYLFNS------------------ 393
Bsu FtsW     MIAIQSFINLGGVSGLIPITGVTLPFISYGGSSLVLLLGSMGILANISMFVKYSENKKKKEPLAPKGMKKKQLKKTVYL 403
Lmo0421      LFTVPACWNILMGLGIVPIMVVPLPFISYGGSMLLVYAALLGLILNVYRRKDIVESTLVN------------------ 416
FtsW1        LIAIQAFINLGGASGLIPLTGVTLPFISYGGSSLMVLSMMLGIVANISMFTKYQRVYKADGSTK--ELPKKQKRR---- 402
RodA1        MLMFHVLENVGMNIGLLPITGIPLPFISYGGSALLGNMMAVGLVLGIRFNFKKSMFEVKEENHAS-------------- 391
RodA2        MILFHVLENIGMTIGLLPITGIPLLFVSYGGSSLLGAFMALGLVLSARYNAPEVNLGKENRF----------------- 389
RodA3        SFAFNIFENIGMTVGLMPLTGIPLPFISYGGSAVLGNFIAVGVVLAIIRSDADLIEEK--------------------- 369
FtsW2        WVSVQMFLNLGGVSGIIPLTGVPLPFISYGGSSVVMLSCAVGFVLAAARRNVL-----------------AKTREVVYL 376
              . .    *:    *::*:  : * *:*****  :     .*.:
```

Figure S1: Sequence alignment of FtsW and RodA proteins from *B. subtilis* and *L. monocytogenes*. The alignment was created using Clustal Omega (Sievers et al., 2011). Based on a study by Meeske *et al.,* amino acid residues of *B. subtilis* RodA that are essential for RodA function are colored in blue, where conservative replacements are possible in

yellow and amino acids that can be changed to certain other amino acids are colored in orange (Meeske et al., 2016).

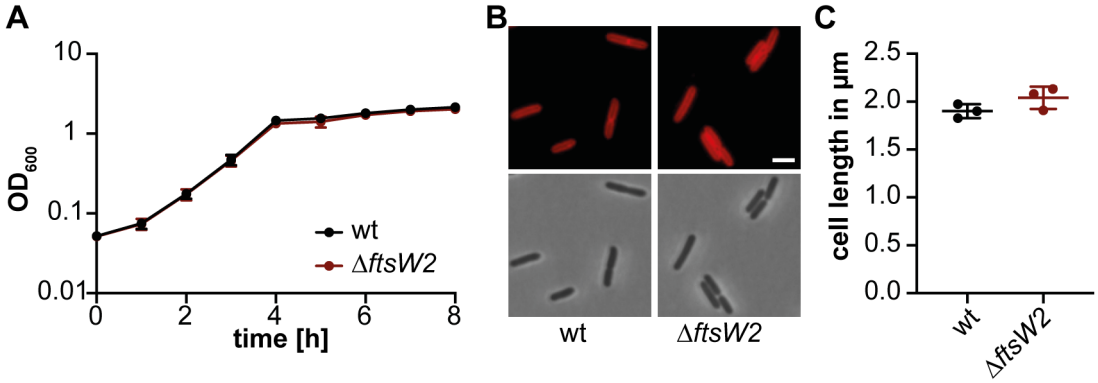

Figure S2: An *L. monocytogenes ftsW2* mutant does not show a growth or cell length defect. (A) Growth of *L. monocytogenes* strains 10403S (wt) and 10403SΔ*ftsW2* in BHI broth at 37°C. (B) Microscopy images of wildtype and *ftsW2* mutant *L. monocytogenes* strains. Bacteria from cultures of the strains described in panel A were stained with the membrane dye nile red and analyzed by fluorescence and phase contrast microscopy. Scale bar is 2 µm. (C) Cell length measurement. The cell length of 300 cells of strain 10403S (wt) and 10403SΔ*ftsW2* was measured and the median cell length calculated and plotted. Three independent experiments were performed, and the average and standard deviation of the median cell length plotted.

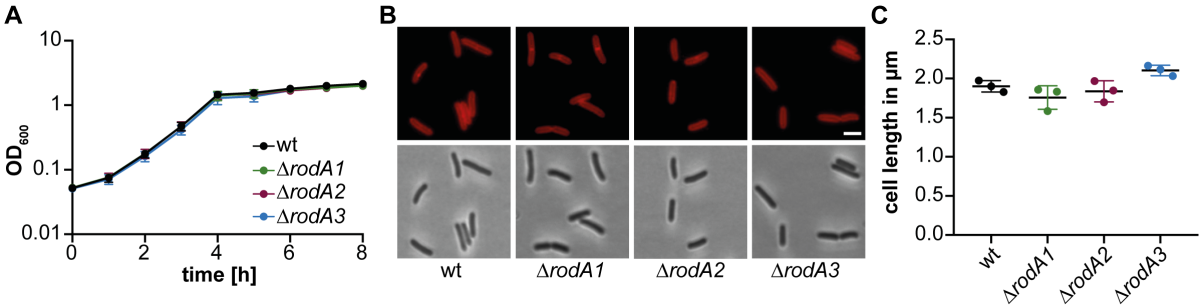

Figure S3: Single *rodA1, rodA2* or *rodA3 L. monocytogenes* strains do not show a growth or cell length defect. (A) Growth of *L. monocytogenes* 10403S (wt), 10403SΔ*rodA1*, 10403SΔ*rodA2* and 10403SΔ*rodA3* in BHI broth at 37°C. (B) Microscopy images of wildtype and mutant *L. monocytogenes* strains. Bacteria from cultures of the strains described in panel A were stained with the membrane dye nile red and analyzed by fluorescence and phase contrast microscopy. Scale bar is 2 µm. (C) Cell length of *L. monocytogenes* wt and *rodA* single mutants. The cell length of 300 cells per strain was measured and the median cell length calculated and plotted. Three independent experiments were performed, and the average and standard deviation of the median cell length plotted.

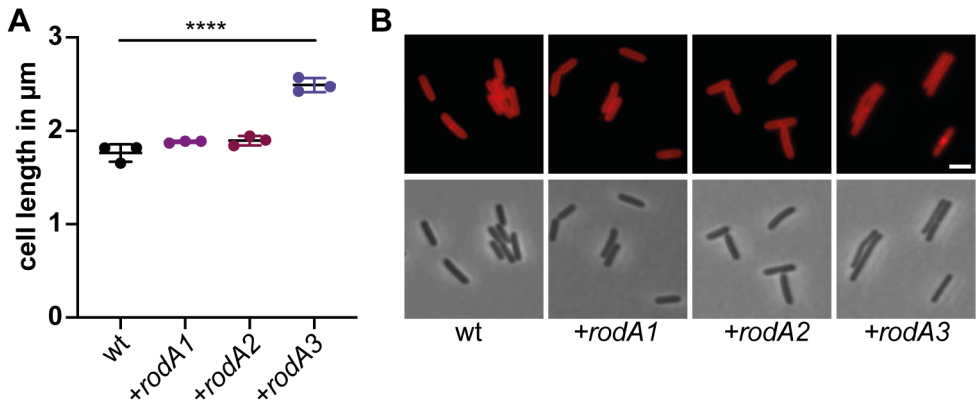

Figure S4: Overexpression of RodA3 results in cell elongation. (A) Cell lengths measurements of 10403S (wt) and strains 10403S pIMK3-*rodA1*, 10403S pIMK3-*rodA2* and 10403S pIMK3-*rodA3*. The cell length of 300 cells per strain was measured. Three independent experiments were performed, and the average and standard deviation of the median cell length plotted. For statistical analysis, a one-way ANOVA coupled with a Dunnett's multiple comparisons test was performed (**** $p \leq 0.0001$). (B) Microscopy images of *L. monocytogenes* strains. Bacteria from cultures of the strains described in panel A were stained with the membrane dye nile red and analyzed by fluorescence and phase contrast microscopy. Scale bar is 2 µm.

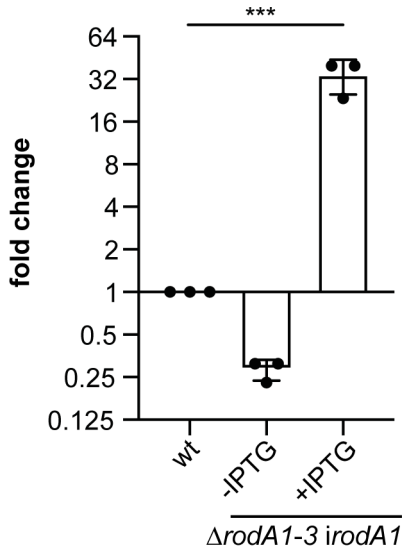

Fig. S5: *rodA1* transcripts are still detected even after prolonged RodA1 depletion. Analysis of *rodA1* expression using qRT-PCR. RNA was isolated from strains 10403S and 10403SΔ*rodA1-3* i*rodA1,* that had been grown in absence and presence of IPTG. Expression of *rodA1* was normalized to the expression of *gyrB* and fold changes calculated using the ΔΔCt method. Averages and standard deviations of three independent experiments were plotted. For statistical analysis, a one-way ANOVA coupled with a Dunnett's multiple comparisons test was performed (*** $p \leq 0.001$).

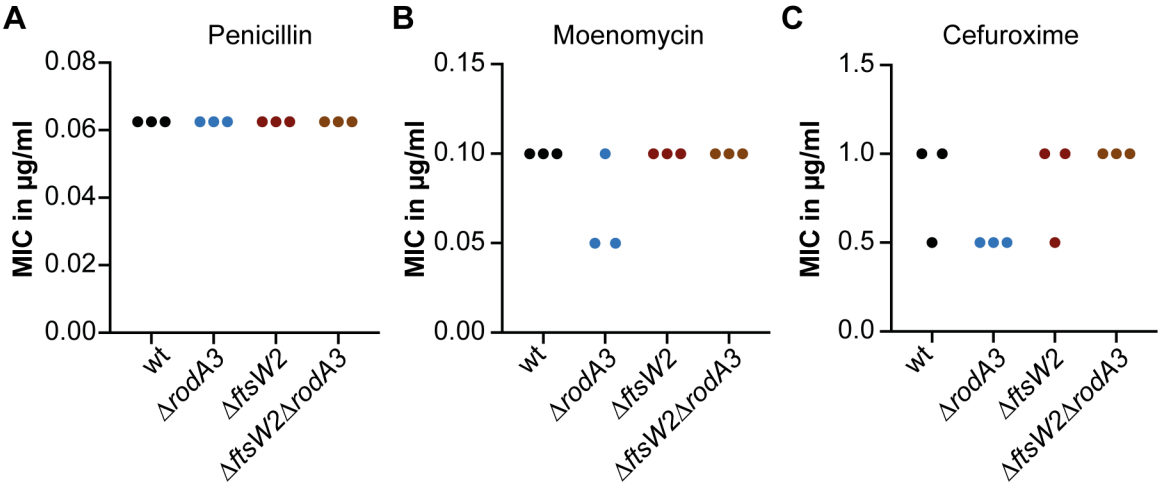

Figure S6: Deletion of *rodA3* but not *ftsW2* has a minor impact on the resistance towards a selected number of cell wall active antibiotics. The minimal inhibitory concentrations for the antibiotics penicillin G (A), moenomycin (B) and cefuroxime (C) were determined for the wildtype *L. monocytogenes* strain 10403S, the 10403SΔ*rodA3* and 10403SΔ*ftsW2* single deletion strains and the 10403SΔ*ftsW2*Δ*rodA3* double mutant strain using a microbroth dilution assay. The result of three biological replicates are shown in A-C.